

Relaxation in scalar gravitational field theory

Riccardo Fantoni

January 20, 2025

Contents

1	Motivations	3
2	Introduction	5
3	Statement of the problem	11
3.1	Basic Equations	11
3.2	The problem	12
3.3	Initial condition	13
3.4	Conserved integrals	15
3.5	Monopole radiation	17
3.6	Analytic results	20
3.6.1	Newtonian limit	20
3.6.2	Relaxation to virial equilibrium	21
3.6.3	Explosion	23
4	Approximations	25
4.1	Quasistatic approximation	25
4.2	Characteristics approximation	29
5	Exact Numerical Integration	31
5.1	Characteristics method	31
5.2	High resolution method	31
6	Numerical results	35
6.1	Relaxation to virial equilibrium	35
6.2	Comparison with the analytic method	35
6.3	Monopole radiation	36
6.4	Quasistatic approximation	36
7	Conclusions	41

<i>CONTENTS</i>	1
A Energy loss in the static approximation	43
A.1 Newtonian approximation	44
B Method of Images	47
C The nonhomogeneous wave equation	49
D The code	53

Chapter 1

Motivations

In this report we want to predict the approach to equilibrium of a spherically symmetric field-particle system initially excited in a non-equilibrium state where the particle is in an unstable circular orbit around the origin [1].

In particular we will be concerned with the realization of a quasistatic approximation to the exact dynamical problem. As the newly built gravitational wave detectors are preparing to receive their first set of data, theoretical efforts are being carried on to solve exactly Einstein's equation to be able to timely interpret such data. Our quasistatic approximation in an unstable circular orbit could become an important tool in the event that such theoretical efforts fail to solve the exact problem in time. The approximation should be particularly useful in interpreting the waveform coming from slowly decaying binary neutron stars.

Binary neutron stars are known to exist and for some of the systems in our own galaxy (like the relativistic binary radio pulsar PSR B1913+16 and PSR B1534+12) general relativistic effects in the binary orbit have been measured to high precision. With the construction of laser interferometers well underway, it is of growing urgency that we be able to predict theoretically the gravitational waveform emitted during the inspiral and the final coalescence of the two stars. Relativistic binary systems, like binary neutron stars and binary black holes pose a fundamental challenge to theorists, as the two-body problem is one of the outstanding unsolved problems in classical general relativity.

Chapter 2

Introduction

When studying a two body problem one decomposes it in the trivial problem involving the center of mass motion and the harder one involving the relative motion of the two masses. Is the second one, we want to focus on. Since we don't want to deal with all the difficulties of General Relativity (there is no analytic solution to the two body problem in GR) and we want to have a more realistic theory than the Newtonian one, we choose to employ a theory which describes gravitation by a nonlinear scalar gravitational field Φ in special relativity. To describe the relative motion in a two body problem we just need one particle moving around the origin. The particle motion is confined at all times in its orbital plane, and its position there is determined by the distance from the origin r_p , and the azimuthal angle ϕ_p . To follow the dynamical evolution of the field-particle system in scalar gravity, one needs to solve a single hyperbolic partial differential equation describing the field evolution, coupled to a system of two ordinary differential equations describing the particle motion,

$$\boxed{\begin{cases} \Phi(\mathbf{r}, t) = \text{source} & , \\ \ddot{r}_p = \dots & , \\ \ddot{\phi}_p = \dots & . \end{cases}} \quad (2.1)$$

The source term of the field equation is where the coupling between the field and the particle dynamics takes place, and is responsible for the nonlinearity of the problem: $\text{source} \sim \exp(\Phi)\rho$, where $\rho(\mathbf{r}, t) = (m/\gamma)\delta(\mathbf{r} - \mathbf{r}_p(t))$ is the comoving matter density, m the particle rest mass, and γ the Lorentz factor.

In particular we want to study the even simpler, spherically symmetric problem. It is infact a peculiarity of scalar gravitation that of being able to generate gravitational waves even in spherical symmetry. This allows the study of wave generation and propagation with the use of just one spatial dimension plus time. In spherical symmetry the particle angular momentum \tilde{u}_ϕ is conserved. There

are then three important quantities in our problem: the initial distance from the origin r_i , the particle rest mass m , and its angular momentum \tilde{u}_ϕ . Two adimensional combinations of these quantities are particularly important to parametrize the problem:

- (1) The initial compaction $\alpha = r_i/m$ which tunes the nonlinearity of the problem:
 - $\alpha \gg 1$ The system is in a weak field and slow particle velocity regime. Newtonian gravitation provides a good analytical approximation to the nearly linear and periodic system.
 - $\alpha \sim 1$ The system is nonlinear and aperiodic. There is no analytic solution to the coupled equations (2.1), and a numerical integration is needed. In this report we will describe an approximate solution which works well when the system relaxes slowly.
- (2) An adimensional measure of the particle angular momentum $J = \tilde{u}_\phi/(\tilde{u}_\phi)_{circ}(r_i)$. Here we are indicating with $(\tilde{u}_\phi)_{circ}(r_i)$ the angular momentum that the particle should have in order to be in a circular orbit at the initial radius r_i .
 - $J = 0$ The particle collapses to the origin.
 - $J = 1$ The particle is in a stable circular orbit. Even though the particle is in circular motion around the origin, it doesn't lose energy by gravitational radiation because in spherical symmetry the particle in circular orbit represents a stationary spherical mass shell.
 - $J > 1$ The particle is initially at the periastron of its elliptical orbit. There is a value J_e such that if $J > J_e$ the particle escapes to infinity, if $J < J_e$ the particle orbit becomes circular at $t = \infty$, and of radius r_e bigger than r_i .

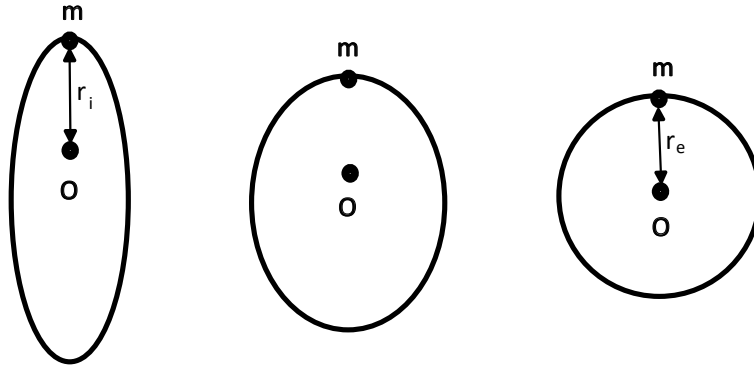


Figure 2.1: Pictorial evolution of the particle orbit when $J > 1$.

$J < 1$ The particle is initially at the apastron of its elliptical orbit. The particle orbit becomes circular at $t = \infty$, and of radius r_e smaller than r_i . If $J \ll 1$ the shell relaxation will be fast (it will reach r_e in a small number of oscillations) and the quasistatic approximation that we are now going to describe will break down.

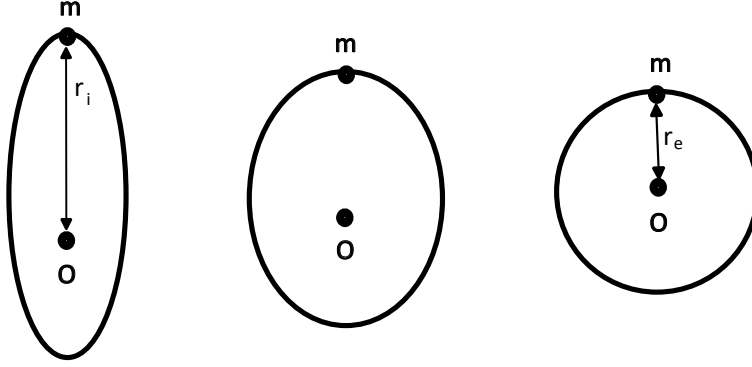


Figure 2.2: Pictorial evolution of the particle orbit when $J < 1$.

When the timescale of orbital decay by radiation is much longer than the orbital period, the particle can be considered to be in “quasiequilibrium”. When this condition is satisfied we are allowed to drop the $\Phi_{,tt}$ (radiative) term from the field equation. Doing this the problem reduces to the solution of three ordinary differential equations which can be solved “analytically”. We will call this simpler problem the “static” approximation to the exact problem,

$$\begin{cases} \nabla^2 \Phi = \text{source} & , \\ \ddot{r}_p = \dots & , \\ \dot{\phi}_p = \dots & . \end{cases} \quad (2.2)$$

In the static approximation (which reduces to Newtonian gravity in the limit $\alpha \gg 1$) the particle motion is conservative but not necessarily periodic due to the nonlinearity of the problem.

Monitoring the exact solution for the field at a fixed radius r_{out} far from the particle, one expects a behaviour similar to the one shown in figure 2.3. In particular the damping of the wave amplitude is due to the fact that the particle is gradually approaching a circular orbit. In the static approximation the field cannot have any damping because of the conservativeness of the particle motion, and we get a behaviour as shown in figure 2.4.

Any reasonable approximation to the exact solution in the nonlinear regime has to be able to reproduce the damping of the wave. The “quasistatic” approximation

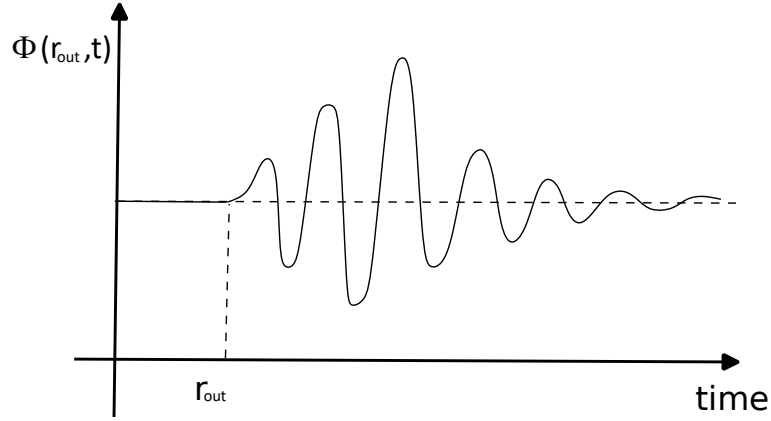


Figure 2.3: Expected behaviour for $\Phi(r_{out}, t)$ as a function of time.

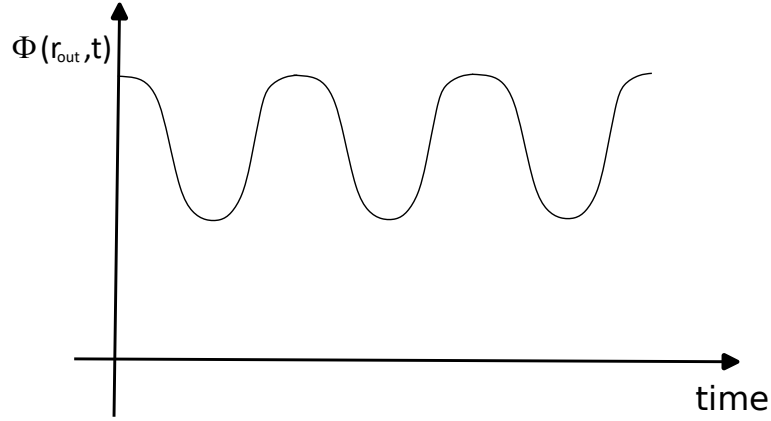


Figure 2.4: Same as figure 2.3 but in the static approximation.

that we propose takes into account the wave damping through the following four steps:

- (1) We use the solution $r_p(t)$ to the static approximation to determine the field equation source term. We then solve the full field equation,

$$\boxed{\Phi(\mathbf{r}, t) = \text{source}} \quad , \quad (2.3)$$

$$(2.4)$$

to find the flux of field energy ($\sim r^2 \Phi_{,t} \Phi_{,r}$) radiated out by the gravity wave. This will allow us to determine the rate of change of the total energy E of

the particle-field system, with respect to time,

$$\frac{dE}{dt} = - \int \text{flux } da \quad . \quad (2.5)$$

- (2) Consider the particle-field system in the stationary state where the particle is in a circular orbit at a radius R . Then instantaneously change the particle angular momentum from $J = 1$ to $J = \tilde{u}_\phi / (\tilde{u}_\phi)_{\text{circ}}(R)$ and calculate the total energy of the system. Repeating this for all radii R between r_i and r_e we get a curve $E(R)$ similar to the one shown in figure 2.5. The values $E(r_e)$ and $E(r_i)$ are exact, while at the true inversion points r_{inv} of the particle orbit, $E(r_{\text{inv}})$ are expected to be good approximations to the corresponding exact values. Knowing $E(R)$ we can find the rate of change of E with respect to R .

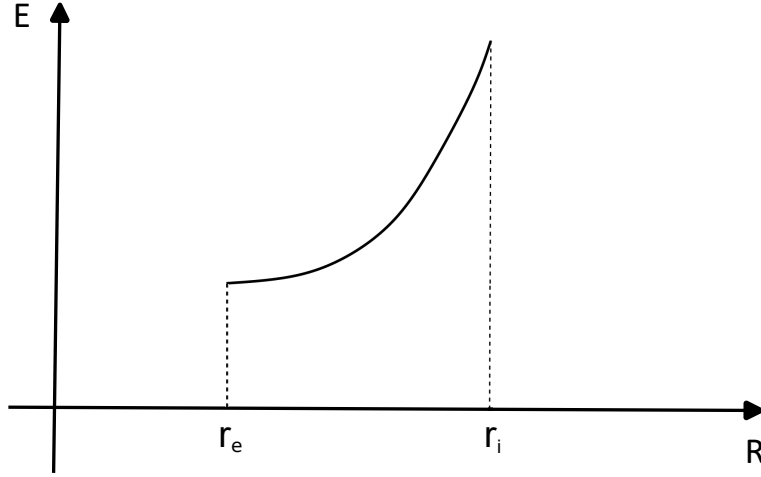


Figure 2.5: Shows the expected behaviour for the total energy of the system E as a function of the circular orbits radii R . The energy curve has its minimum at r_e , the radius of the circular orbit on which the particle decays at $t = \infty$.

- (3) Use the chain rule to get the rate of change of R with respect to time,

$$\frac{dR}{dt} = \frac{dE/dt}{dE/dR} \quad . \quad (2.6)$$

- (4) Finally knowing dR/dt we can correct the previous static estimate of the field equation source term. We can then solve the full field equation again to get the wave damping.

Chapter 3

Statement of the problem

3.1 Basic Equations

The gravitational field is described by a massless scalar field $\Phi(x^\alpha)$ in special relativity. The scalar field does not modify the background space-time geometry which is always Minkowskian. Consider a particle of rest mass m moving along a world-line $z^\alpha(\lambda)$. Then the action for the field-particle system is,

$$I = \int \mathcal{L} (-g)^{1/2} d^4x \quad , \quad (3.1)$$

where the lagrangian density \mathcal{L} is,

$$\mathcal{L} = -\frac{1}{8\pi G} g^{\alpha\beta} \Phi_{,\alpha} \Phi_{,\beta} - \rho e^\Phi \quad , \quad (3.2)$$

and where the comoving density is,

$$\rho = m \int \left(-g_{\alpha\beta} \frac{dz^\alpha}{d\lambda} \frac{dz^\beta}{d\lambda} \right)^{1/2} \delta^4(\vec{x} - \vec{z}(\lambda)) (-g)^{-1/2} d\lambda \quad . \quad (3.3)$$

Here the metric tensor $g_{\alpha\beta}$ is the usual Minkowski metric $\eta_{\alpha\beta}$ since space-time is flat in this theory [i.e. $g_{\alpha\beta} = \eta_{\alpha\beta} = \text{diag}(-1, 1, 1, 1)$ in Cartesian coordinates]. We use arrows to denote four-vectors and boldface to denote three-vectors. We will set the speed of light $c = 1$ but will display the gravitational coupling constant (Newton's constant) G explicitly. If we choose λ equal to the proper time τ along the particle world-line, then,

$$\rho = m \int \delta^4(\vec{x} - \vec{z}(\tau)) (-g)^{-1/2} d\tau \quad (3.4)$$

$$= \frac{m}{\gamma} \delta^3(\mathbf{x} - \mathbf{z}(t)) (-g)^{-1/2} \quad , \quad (3.5)$$

where $\gamma \equiv dz^0/d\tau$ is the Lorentz factor.

Varying the Lagrangian (3.2) with respect to Φ gives the field equation of motion,

$$\boxed{\Phi = 4\pi G e^\Phi \rho} \quad . \quad (3.6)$$

In the Newtonian limit, where $\Phi \ll 1$, equation (3.6) becomes linear and reduces to Poisson's equation. Varying the lagrangian with respect to z^α gives the particle equation of motion,

$$\frac{D^2 z^\alpha}{d\tau^2} + \left[g^{\alpha\beta} + \frac{dz^\alpha}{d\tau} \frac{dz^\beta}{d\tau} \right] \Phi_{,\beta} = 0 \quad , \quad (3.7)$$

where D denotes covariant differentiation. Here we are allowing for curvilinear coordinates; covariant differentiation reduces to ordinary differentiation in Cartesian coordinates. In the non relativistic limit equation (3.7) implies that the gravitational force is $-\nabla\Phi$. The fully relativistic form ensures that the four-velocity $u^\alpha = dz^\alpha/d\tau$ remains orthogonal to the four-acceleration $a^\alpha = Du^\alpha/d\tau$.

3.2 The problem

Consider one particle of rest mass m moving along a world-line $z^\alpha(\tau) = (\mathbf{r}_p, t)$ with four-velocity u^α , under the influence of a massless scalar gravitational field $\Phi(\mathbf{r}, t)$ in special relativity. In spherical symmetry the comoving matter density takes the form,

$$\rho(r, t) = \frac{m/\gamma}{4\pi r_p^2(t)} \delta(r - r_p(t)) \quad , \quad (3.8)$$

where $r = |\mathbf{r}|$ and $\gamma = u^0$ is the Lorentz factor. The particle effectively represents an entire spherical shell of radius r_p and mass surface density $\sigma = m/(\gamma 4\pi r_p^2)$.

Assuming the particle confined in the $\theta = \pi/2$ plane, so that $u^\theta = 0$ at all times, the equations of motion in spherical coordinates $\mathbf{r}_p = (r_p, \theta_p, \phi_p)$, are,

$$\left\{ \begin{array}{l} \dot{r}_p = \frac{\tilde{u}_r}{\tilde{u}^0} \\ \dot{\psi} = \frac{\tilde{u}_\phi^2}{\tilde{u}^0 r_p^3} - \frac{e^{2\Phi} \Phi_{,r}}{\tilde{u}^0} \end{array} \right. , \quad \left\{ \begin{array}{l} r_p^2 \dot{\phi}_p = \frac{\tilde{u}_\phi}{\tilde{u}^0} \\ \dot{\psi} = 0 \end{array} \right. , \quad (3.9)$$

where,

$$\tilde{u}^0 = \sqrt{e^{2\Phi} + \tilde{u}_r^2 + \tilde{u}_\phi^2/r_p^2} \quad , \quad (3.10)$$

$$\tilde{u}^\alpha \equiv e^\Phi u^\alpha \quad , \quad (3.11)$$

and we use the dot to denote total differentiation with respect to time, and commas to indicate partial differentiation.

The particle moves conserving its orbital angular momentum \tilde{u}_ϕ . For a static gravitational field the particle energy \tilde{u}^0 is also a constant.

Notice that from the field equation (3.6) follows that $\phi_{,r}$ has, at all times ¹, a jump of $4\pi G e^\Phi \sigma$ at the shell surface $r = r_p(t)$. It is then necessary to specify how we calculate the gravitational force felt by the shell. We will use in equation (3.9),

$$\Phi_{,r} \equiv [\Phi_{,r}(r_p-) + \Phi_{,r}(r_p+)]/2 . \quad (3.12)$$

In this way we prevent any small patch of surface on the shell from interacting with itself.

3.3 Initial condition

The field starts from a moment of time symmetry, so that at $t = 0$,

$$\begin{aligned} \Phi_{,t} &= 0 , \\ \nabla^2 \Phi &= 4\pi G e^\Phi \sigma \delta(r - r_i) , \end{aligned} \quad (3.13)$$

where $r_i = r_p(t = 0)$ is the initial shell radius. The field is subject to the boundary conditions,

$$\Phi_{,r} = 0 \quad r = 0 , \quad (3.14)$$

$$(r\Phi)_{,r} = 0 \quad r \rightarrow \infty . \quad (3.15)$$

Choosing,

$$\Phi = \begin{cases} a/r_p & r \leq r_p \\ a/r & r > r_p \end{cases} , \quad (3.16)$$

we can determine $a_i = a(t = 0)$ from the matching condition at the shell's surface,

$$\Phi_{,r}(r_p+) - \Phi_{,r}(r_p-) = \frac{Gm e^{2\Phi}}{r_p^2 \tilde{u}^0} . \quad (3.17)$$

Initially the particle is in a circular orbit of radius r_i around the origin,

$$\begin{aligned} \tilde{u}_r &= 0 , \\ r_i (u_{circ}^\phi)^2 &= [\Phi_{,r}(r_i-) + \Phi_{,r}(r_i+)]/2 = -\frac{a_i}{2r_i^2} , \end{aligned} \quad (3.18)$$

¹We can safely assume that $\Phi_{,tt}$ remains finite at all times at the shell surface.

with an angular momentum,

$$(\tilde{u}_\phi)_{circ} = e^\Phi r_i^2 u_{circ}^\phi = e^{a_i/r_i} \sqrt{-\frac{a_i r_i}{2}} . \quad (3.19)$$

We can then find a_i from equation (3.17), which becomes,

$$a_i = -\frac{Gm e^{a_i/r_i}}{\sqrt{1 - a_i/(2r_i)}} . \quad (3.20)$$

This initial condition (an Einstein state) is a stationary wave for the field equation of motion and a stable circular orbit for the particle. So if we let the system evolve from this initial state nothing will happen: the particle will keep moving in the circular orbit at radius $r_p(t) = r_i$ under the influence of the static gravitational field (3.16). This can be shown, for example, rewriting the field equation of motion in terms of the auxiliary functions,

$$\begin{aligned} X(r, t) &= [(r\Phi)_{,r} + (r\Phi)_{,t}]/2 , \\ Y(r, t) &= [(r\Phi)_{,r} - (r\Phi)_{,t}]/2 . \end{aligned} \quad (3.21)$$

Now equation (3.6) becomes,

$$\begin{aligned} X_{,t} &= X_{,r} - F\delta(r - r_p) , \\ Y_{,t} &= -Y_{,r} + F\delta(r - r_p) , \end{aligned} \quad (3.22)$$

where $F = Gm \exp(2\Phi)/(2r_p \tilde{u}^0)$. The initial condition for X and Y becomes,

$$X(r, 0) = Y(r, 0) = \begin{cases} a_i/(2r_i) & -r_i < r < r_i \\ 0 & \text{otherwise} \end{cases} , \quad (3.23)$$

From equations (3.19) and (3.20) follows that when $\xi = 1$, at $t = 0$, the source term $F = a_i/(2r_i)$. So that after an infinitesimal timestep dt , $X(r, dt) = X(r, 0)$ and $Y(r, dt) = Y(r, 0)$.

So we perturb the system changing the particle's angular momentum by a factor ξ ,

$$\tilde{u}_\phi = \xi (\tilde{u}_\phi)_{circ} , \quad (3.24)$$

and let it evolve.

3.4 Conserved integrals

The particle-field dynamical system is characterized by a time-varying matter and velocity profile, interacting with a time varying scalar field containing radiation. Conservation of energy-momentum follows from,

$$\nabla T = 0 \quad , \quad (3.25)$$

where T is the total stress-energy tensor of the system,

$$T^{\mu\nu} = \frac{2}{(-g)^{1/2}} \frac{\delta[\mathcal{L}(-g)^{1/2}]}{\delta g_{\mu\nu}} \quad . \quad (3.26)$$

Carrying out the variation using equation (3.2) we find,

$$T_{\mu\nu} = T_{\mu\nu}^{field} + T_{\mu\nu}^{particle} \quad , \quad (3.27)$$

where,

$$T_{\mu\nu}^{field} = \frac{1}{4\pi G} [\Phi_{,\mu} \Phi_{,\nu} - \frac{1}{2} g_{\mu\nu} \Phi^{,\alpha} \Phi_{,\alpha}] \quad , \quad (3.28)$$

$$T_{\mu\nu}^{particle} = \rho e^{\Phi} u_{\mu} u_{\nu} \quad . \quad (3.29)$$

Conservation of energy-momentum gives rise to the following conserved integrals,

$$\frac{\partial}{\partial t} \int_{S_r} T^{\mu 0}(\mathbf{x}, t) d^3x = - \int T^{\mu i}{}_{,i} d^3x = -4\pi r^2 T^{\mu r}(r, t) \quad , \quad (3.30)$$

where S_r is the volume of the sphere of radius r centered at the origin, and we used spherical symmetry in the last equality.

When $r > r_p(t)$ we find,

$$[\mu = 0] \quad \frac{\partial}{\partial t} \left\{ \frac{1}{2G} \int_0^r [(\Phi_{,0})^2 + (\Phi_{,r})^2] r^2 dr + m \tilde{u}^0 \right\} = \frac{1}{G} r^2 \Phi_{,0} \Phi_{,r} \quad , \quad (3.31)$$

$$[\mu = \phi] \quad \frac{\partial}{\partial t} \left(\frac{\tilde{u}_{\phi}}{r_p^2} \right) = 0 \quad ,$$

$$[\mu = r] \quad \frac{\partial}{\partial t} \left\{ \frac{1}{G} \int_0^r \Phi_{,0} \Phi_{,r} r^2 dr - m \tilde{u}_r \right\} = \frac{1}{2G} r^2 [(\Phi_{,0})^2 + (\Phi_{,r})^2] \quad ,$$

The particle-field total mass energy is given by the integral in equation (3.31),

$$E = E^{field} + E^{particle} \quad , \quad (3.32)$$

$$E^{field} = \frac{1}{2G} \int_0^r [(\Phi_{,0})^2 + (\Phi_{,r})^2] r^2 dr \quad ,$$

$$E^{particle} = m \tilde{u}^0 \quad .$$

According to equation (3.31), when evaluated at large enough radius, outside any radiation or matter, E is conserved. As the particle shell breaths around its asymptotic virial equilibrium state, $E^{particle}$ will undergo exponentially dumped oscillations around its asymptotic value (see figure 3.1): the oscillations are due to the coupling with the field, and the dumping to the gravitational radiation going out to infinity (as a gravity wave). So that after a long time, apart from some particular combinations of ξ and r_i/m (see section 3.6.2), some energy will have been exchanged between the field and the particle.

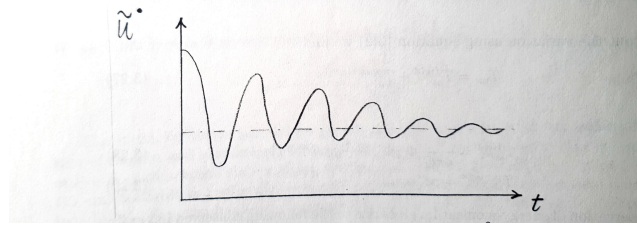


Figure 3.1: Shows the expected behaviour of the particle energy \tilde{u}^0 as a function of time for the case $\alpha \sim 1$ and $\xi < 1$.

For a static situation, the $(\Phi_{,r})^2$ term in equation (3.32) can be integrated by parts to get,

$$E = -\frac{m\Phi_p e^{2\Phi_p}}{2\tilde{u}^0} + m\tilde{u}^0, \quad (3.33)$$

where $\Phi_p = \Phi(r_p, t)$. In the Newtonian limit equation (3.33) becomes,

$$\begin{aligned} E &= m \left[-\frac{\Phi_p}{2} + \dots + (1 + \Phi_p + \dots) \left(1 + \frac{v_r^2}{2} + \frac{v_\phi^2}{2r^2} + \dots \right) \right] \\ &\approx m \left(1 + \frac{v_r^2}{2} + \frac{v_\phi^2}{2r^2} + \frac{\Phi_p}{2} \right), \end{aligned} \quad (3.34)$$

where $v_i \equiv u_i/u^0$. So E is the sum of the rest mass, plus the kinetic energy, plus the gravitational potential energy of the matter shell.

When $r < r_p(t)$,

$$[\mu = 0] \quad \frac{\partial}{\partial t} \int_0^r [(\Phi_{,0})^2 + (\Phi_{,r})^2] r^2 dr = 2r^2 \Phi_{,0} \Phi_{,r}, \quad (3.35)$$

$$[\mu = \phi] \quad 0 = 0, \quad (3.36)$$

$$[\mu = r] \quad \frac{\partial}{\partial t} \int_0^r \Phi_{,0} \Phi_{,r} r^2 dr = \frac{r^2}{2} [(\Phi_{,0})^2 + (\Phi_{,r})^2], \quad (3.37)$$

which implies,

$$(\Phi_{,0})^2 = (\Phi_{,r})^2 \quad \forall t \quad \forall r < r_p(t) \quad . \quad (3.38)$$

Those conserved integrals can be used as self consistent checks on our numerical integration. In figure 3.2 we show what we would expect if we were to evaluate the energy conservation equation,

$$\begin{aligned} & \int_0^{r_{ec}} [(\Phi_{,0})^2 + (\Phi_{,r})^2] r^2 dr + 2m\tilde{u}^0 \theta(r_{ec} - r_p(t)) \\ & - 2 \int_0^t dt [\Phi_{,0} \Phi_{,r} r_{ec}^2 - m\delta(r_{ec} - r_p(t)) \tilde{u}_r] = \\ & \int_0^{r_{ec}} (\Phi(r, 0)_{,r} r)^2 dr + 2m\tilde{u}^0(t=0) \theta(r_{ec} - r_p(0)) \quad . \end{aligned} \quad (3.39)$$

as a function of time at two fixed radii r_{ec} . The first radius is inside the shell at all times, the second is always in the vacuum exterior. In the first case the right hand side of equation (3.39) is zero, the integrated flux term (second integral in equation (3.39)) is large, and the energy conservation involves the cancellation of large terms. Consequently, the high degree to which we are able to maintain energy conservation is a nontrivial measure of the accuracy of the code. In the exterior, the flux is small and energy conservation is not a stringent test.

3.5 Monopole radiation

In the weak field, slow motion limit, the radiation field can be obtained by a multipole expansion. Since the theory involves a scalar field, the lowest-order contribution to the radiation comes from the monopole term. This is in contrast with electromagnetism (vector field: dipole radiation) or general relativity (tensor field: quadrupole radiation).

Using Green's function for the wave equation we can transform equation (3.6) into the integral form,

$$\Phi(\mathbf{x}, t) = -G \int d^3x' \frac{[e^\Phi \rho]_{t'=t-|\mathbf{x}-\mathbf{x}'|}}{|\mathbf{x} - \mathbf{x}'|} \quad . \quad (3.40)$$

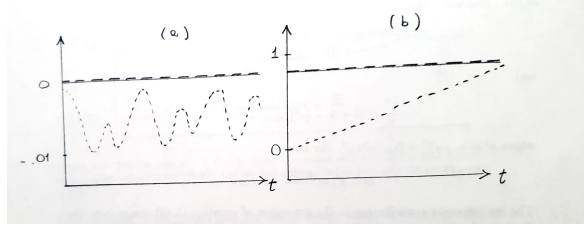


Figure 3.2: Energy conservation at two selected radii as a function of time. The solid line shows the left-hand side of equation (3.39) (volume integral plus integrated flux), the dotted line shows the second term alone (integrated flux), and the dashed line shows the right-hand side (volume integral at $t = 0$). The radii are (a) $r_{ec} < r_p(t)$ at all times, (b) $r_{ec} > r_p(t)$ at all times. The degree to which the solid and dashed lines coincide compared with the magnitude of the dotted line is a measure of the code's ability to conserve energy.

In the wave zone we can replace the denominator in equation (3.40) by the distance $r = |\mathbf{x}|$. To isolate the conserved rest mass m , define the rest density to be,

$$\rho_0 = \gamma \rho \quad . \quad (3.41)$$

Then,

$$\Phi(\mathbf{x}, t) \approx -\frac{G}{r} \int d^3x' \left[\frac{e^\Phi}{\gamma} \rho_0 \right]_{t'=t-|\mathbf{x}-\mathbf{x}'|} \quad . \quad (3.42)$$

In the integrand, expand,

$$\begin{aligned} \rho_0(\mathbf{x}', t') &= \rho_0(\mathbf{x}', t-r) + (r - |\mathbf{x} - \mathbf{x}'|) \rho_{0,t} \\ &\quad + \frac{1}{2} (r - |\mathbf{x} - \mathbf{x}'|)^2 \rho_{0,tt} + \dots \quad , \end{aligned} \quad (3.43)$$

and,

$$\frac{e^\Phi}{\gamma} = [1 + \Phi - \frac{1}{2}v^2]_{t'=t-r} + \dots \quad , \quad (3.44)$$

where $v^2 = [u_r/u^0]^2 + [u_\phi/(u^0 r)]^2$. For large r ,

$$r - |\mathbf{x} - \mathbf{x}'| \approx \frac{\mathbf{x} \cdot \mathbf{x}'}{r} = r' \cos \theta' \quad . \quad (3.45)$$

The leading-order contribution to the expansion of equation (3.42) comes from the product of ρ_0 in equation (3.43) with the 1 in equation (3.44). The resulting

integral gives m , so that this term represents the nonradiative Coulomb field. Thus the leading-order radiation field is,

$$\Phi(\mathbf{x}, t) = -\frac{G}{r} \int d^3x' [\rho_0(\Phi - \tfrac{1}{2}v^2) + r' \cos \theta' \rho_{0,t} + r'^2 \cos^2 \theta' \rho_{0,tt}]_{t-r} . \quad (3.46)$$

To this order, it is irrelevant whether one uses ρ or ρ_0 in equation (3.46).

For a spherically symmetric density distribution, the term proportional to $\cos \theta'$ in equation (3.46) integrates to zero, giving,

$$\Phi(r, t) = -\frac{G}{r} \int dr' 4\pi r'^2 [\rho_0(\Phi - \tfrac{1}{2}v^2) + \tfrac{1}{6}r_p^2 \rho_{0,tt}]_{t-r} . \quad (3.47)$$

The last term in the integrand can be rewritten as follows,

$$\frac{1}{6} \int dr' 4\pi r'^2 \frac{d^2(r'^2)}{dt^2} \rho_0 = \frac{1}{3} m \left(\tilde{u}_r^2 + r_p \frac{d\tilde{u}_r}{dt} \right) , \quad (3.48)$$

and using the equation of motion (3.9) in the weak field limit, we find,

$$\frac{1}{6} \int dr' 4\pi r'^2 \frac{d^2(r'^2)}{dt^2} \rho_0 = \frac{1}{3} m \left(\tilde{u}_r^2 + \frac{\tilde{u}_\phi^2}{r_p^2} - r_p \Phi_{,r} \right) , \quad (3.49)$$

Thus equation (3.47) becomes,

$$r\Phi(r, t) = Gm \left\{ \frac{1}{6} \left[r_p (\Phi_{,r}(r_p+) + \Phi_{,r}(r_p-)) + \tilde{u}_r^2 + \frac{\tilde{u}_\phi^2}{r_p^2} \right] - \Phi \right\}_{t-r} . \quad (3.50)$$

In figure 3.3 we show how a snapshot of the field at $t = t_o$ should look like, and compare it with the leading order radiation field of equation (3.50), in the wave zone.

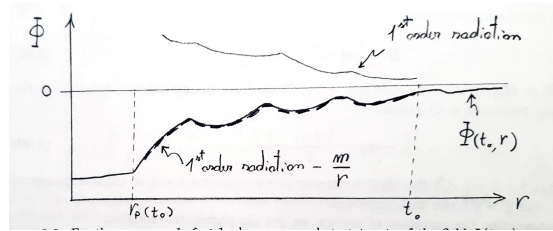


Figure 3.3: For the case $\alpha \sim 1$, $\xi < 1$, shows a snapshot at $t = t_o$ of the field $\Phi(t_o, r)$, the first order radiation part (3.50), and the first order radiation part plus the zeroth order $-m/r$.

From equation (3.31) follows that the rate of energy emission when $r > r_p(t)$ is,

$$\frac{dE}{dt} = -\frac{1}{G}r^2\Phi_{,t}\Phi_{,r} = -\frac{1}{G}(r\Phi_{,t})^2, \quad (3.51)$$

where in the last equality we used the fact that since X is propagating to the left, the following outgoing wave boundary condition must hold,

$$X(r, t) = 0 \quad \text{or} \quad (r\Phi)_{,r} + (r\Phi)_{,t} = 0 \quad \forall t, \quad \forall r > r_p(t). \quad (3.52)$$

3.6 Analytic results

3.6.1 Newtonian limit

For weak fields and slow velocities we can test our code using the analytic solution from Newtonian gravitation. In this limit the particle equation of motion is,

$$\ddot{r}_p = -\Phi_{,r} + \frac{J^2}{r_p^3}, \quad (3.53)$$

$$\Phi_{,r} = \frac{Gm}{2r^2},$$

$$J = (r^2 v_\phi)_{t=0} = r_i^2 \xi \sqrt{\Phi_{,r}(r_i)/r_i} = \xi \sqrt{Gmr_i/2},$$

which can be rewritten as,

$$\begin{aligned} \ddot{x} &= -\frac{M_{eff}}{x^2} + \frac{J_{eff}^2}{x^3}, \\ \dot{x}(0) &= 0, \\ x(0) &= 1, \end{aligned} \quad (3.54)$$

where $r_p(t) = r_i x(t)$, $M_{eff} = Gm/(2r_i^3)$, and $J_{eff} = \xi \sqrt{M_{eff}}$. The first integral yields the conserved energy,

$$E = \frac{1}{2}\dot{x}^2 - \frac{M_{eff}}{x} + \frac{J_{eff}^2}{2x^2}. \quad (3.55)$$

For $E = M_{eff}(\xi^2/2 - 1) < 0$ (i.e. $\xi^2 < 2$) we have bound orbits. Solving for the turning points ($\dot{x} = 0$) yields,

$$x_{\pm} = \frac{1 \pm (1 - \xi^2)}{2 - \xi^2}. \quad (3.56)$$

So that for $0 < \xi < 1$ the shell contracts to $r_i x_-$ and for $1 < \xi < \sqrt{2}$ it expands to $r_i x_-$. For $\xi > \sqrt{2}$ the shell explodes.

Integrating the equation of motion we get the parametric solution,

$$\begin{aligned} x &= a(1 - e \cos(u)) \quad , \\ t &= \frac{P}{2\pi}(u - e \sin(u)) - \frac{P}{2} \quad , \end{aligned} \quad (3.57)$$

where the semimajor axis, eccentricity and period are given by,

$$\begin{aligned} a &= \frac{1}{2 - \xi^2} \quad , \\ e &= |1 - \xi^2| \quad , \\ P &= 2\pi \sqrt{\frac{2r_i^3}{Gm(2 - \xi^2)^3}} \quad . \end{aligned} \quad (3.58)$$

Inserting this analytic solution into equation (3.47) and differentiating with respect to time gives the wave amplitude in the wave zone,

$$r\Phi_{,t} = -\frac{4}{3} \frac{(Gm)^2}{r_i} \left[\frac{\dot{x}}{x^2} \right]_{t-r} \quad . \quad (3.59)$$

From equation (3.51) we get for the rate of energy emission,

$$\frac{dE}{dt} = -\frac{16}{9} \frac{(Gm)^4}{r_i^2} \left[\frac{\dot{x}^2}{x^4} \right]_{t-r} \quad . \quad (3.60)$$

Integrating over an oscillation period we get the energy radiated per period,

$$\Delta_P E = -\frac{16\pi}{36} m \left(\frac{Gm}{r_i} \right)^{7/2} \frac{(1 - \xi^2)^2}{\xi^7} (5 - 2\xi^2 + \xi^4) \quad . \quad (3.61)$$

3.6.2 Relaxation to virial equilibrium

If the shell does not explode or collapse, it will eventually reach, as it loses energy by emitting gravitational waves, an equilibrium circular orbit (see figure 3.4). At this point the particle-field system is in an Einstein state where $\tilde{u}_r = 0$, $\tilde{u}_\phi^2 = r_p^3 e^{2\Phi} \Phi_{,r}$, and the field is static and of the form (3.16), in a neighborhood of the shell.

Given the angular momentum of the particle \tilde{u}_ϕ we can then predict the final equilibrium radius r_e , by solving the following equations in $a_e = a(t = \infty)$ and

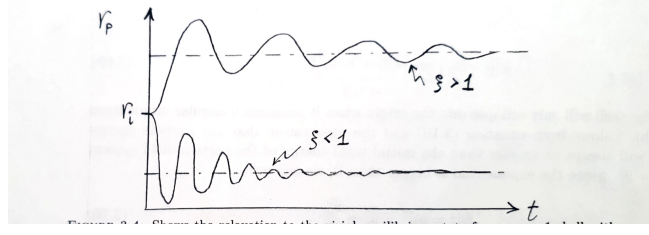


Figure 3.4: Shows the relaxation to the virial equilibrium state for an $\alpha \sim 1$ shell with two different values of ξ : $\xi < 1$ and $\xi > 1$.

$$r_e = r_p(t = \infty),$$

$$a_e = -\frac{Gm e^{2a_e/r_e}}{\sqrt{e^{2a_e/r_e} + \tilde{u}_\phi^2/r_e^2}}, \quad (3.62)$$

$$\tilde{u}_\phi^2 = e^{2a_e/r_e} r_e^3 (-a_e/(2r_e^2)) . \quad (3.63)$$

One can verify that,

$$\begin{cases} r_e < r_i & \text{when } \xi < 1 \\ r_e > r_i & \text{when } \xi > 1 \end{cases} , \quad (3.64)$$

This final state is a virial equilibrium state. Taking the trace of the special relativistic virial theorem,

$$\int T^{ij} d^3x = \frac{1}{2} \frac{\partial^2}{\partial t^2} \int T^{00} x^i x^j d^3x , \quad (3.65)$$

gives at equilibrium,

$$\int \rho e^\Phi (u_r^2 + u_\phi^2/r^2) d^3x = \frac{1}{8\pi G} \int (\nabla \Phi)^2 d^3x = -\frac{1}{2} \int \rho \Phi e^\Phi d^3x , \quad (3.66)$$

or, when $\tilde{u}_r = 0$,

$$\frac{\tilde{u}_\phi^2}{r_e^2} = -\frac{1}{2} e^{2\Phi} \Phi , \quad (3.67)$$

which is the same as equation (3.63), when the field is of the form (3.16).

The final energy of the particle-field system is,

$$E(t = \infty) = -\frac{m}{2} \frac{a}{r_e} \frac{e^{2a/r_e}}{\tilde{u}^0(t = \infty)} + m \tilde{u}^0(t = \infty) , \quad (3.68)$$

where,

$$\tilde{u}^0(t = \infty) = \sqrt{e^{2a_e/r_e} + \frac{\tilde{u}_\phi^2}{r_e^2}} . \quad (3.69)$$

The shell will only collapse into the origin when it possesses 0 angular momentum². This follows from equation (3.10) and the observation that the particle energy $m\tilde{u}^0$ will always be smaller than the initial total energy of the particle-field system $E(t = 0)$. Since the exponential is bigger than 0, we can write,

$$[E(t = 0)]^2 > \tilde{u}_r^2 + \frac{\tilde{u}_\phi^2}{r^2} , \quad (3.70)$$

and when $\tilde{u}_r = 0$, equation (3.70) gives the following lower bound on the accessible radii³,

$$r_p > \tilde{u}_\phi / E(t = 0) , \quad (3.71)$$

where,

$$\begin{aligned} E(t = 0) &= \frac{a^2}{2r_i} + m\tilde{u}^0(t = 0) , \\ \tilde{u}^0(t = 0) &= \sqrt{e^{2a/r_i} + \frac{\tilde{u}_\phi^2}{r_i^2}} . \end{aligned} \quad (3.72)$$

3.6.3 Explosion

In order to explode the shell has to reach $r = \infty$ with at least $\tilde{u}_r = 0$. But for $r \rightarrow \infty$, $\sigma \rightarrow 0$ and $\phi \rightarrow 0$ so that $E^{particle} \rightarrow m$. When the shell is at infinity E^{field} will be a small positive quantity. So for the explosion to happen the initial energy of the particle-field system has to be greater than m ,

$$E(t = 0) > m , \quad (3.73)$$

In the Newtonian limit $r_i \gg m$, condition (3.73) reduces to $\xi > \sqrt{2}$. The escape radial velocity is (see figure 3.5),

$$\begin{aligned} \tilde{u}_r(r \rightarrow \infty) &= \sqrt{[(E(t = 0) - E^{field}(t = \infty))/m]^2 - 1} \\ &\approx \sqrt{[E(t = 0)/m]^2 - 1} , \end{aligned} \quad (3.74)$$

²This is different from what happens in General Relativity where the shell can collapse also for non-zero values of the angular momentum.

³At sufficiently small ξ one can get a better lower bound by substituting $E(t = 0)$ with $\tilde{u}^0(t = 0)$ in equation (3.71).

or,

$$v_r(r \rightarrow \infty) \approx \frac{\sqrt{E^2(t=0) - m^2}}{E(t=0)} . \quad (3.75)$$

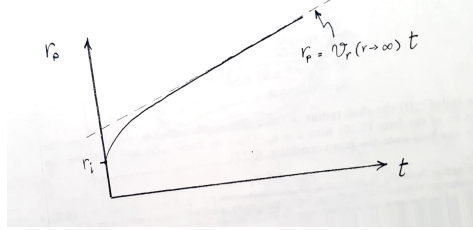


Figure 3.5: Expected shell behaviour for $\xi > \xi_e$.

Chapter 4

Approximations

Here we will describe two approximated solutions of the exact problem stated in chapter 3.

4.1 Quasistatic approximation

When it takes many oscillations for the particle to settle into the final stable circular orbit, we can hope to approximate its slow motion with a quasistatic approximation. The idea is the following. Consider the static version of our problem (equations (3.9)-(3.6)),

$$\begin{aligned} (r\Phi)_{,rr} &= \frac{Gme^{2\Phi}}{\tilde{u}^0 r_s} \delta(r - r_s) \quad , \\ \frac{dr_s}{dt} &= \frac{\tilde{u}_r}{\tilde{u}^0} \quad , \\ \frac{d\tilde{u}_r}{dt} &= \frac{\tilde{u}_\phi^2}{\tilde{u}^0 r_s^3} - \frac{e^{2\Phi}\Phi_{,r}}{\tilde{u}^0} \quad , \\ \tilde{u}^0 &= \sqrt{e^{2\Phi} + \tilde{u}_r^2 + \tilde{u}_\phi^2/r_s^2} \quad , \\ \tilde{u}_\phi &= \text{constant} \quad , \end{aligned} \tag{4.1}$$

where we called $r_s(t)$ the shell radius in this static approximation. At all times the field must be of the form (3.16) with $a = a_s$. Once we know $r_s(t)$ and $\tilde{u}_r(t)$ we can determine the field from the jump condition (3.17),

$$a_s = - \frac{Gm e^{2a_s/r_s}}{\sqrt{e^{2a_s/r_s} + \tilde{u}_r^2 + \tilde{u}_\phi^2/r_s^2}} \quad . \tag{4.2}$$

Since we have a static field $\Phi = \Phi(r, r_s(t), \tilde{u}_r(t))$, $\Phi_{,t} = 0$ and the system is conservative. The shell will then experience undumped oscillations around its

final equilibrium radius r_e . In order to have the shell reach r_e , we need a recipe to dump the oscillations. This will give us a quasistatic approximation to the true shell motion.

Once we know the initial r_i , and final r_e shell radii we can construct a sequence of intermediate “quasi-static” Einstein states as follows. The shell initially at r_i will contract ($\xi < 1$) or expand ($\xi > 1$) towards r_e in a succession of circular orbits ($\tilde{u}_r = 0$) occurring at the true inversion points of the particle trajectory. We call the intermediate radii of these circular orbits, $r_{q.s.}(i) = r_p(P_1 + \dots + P_i)$, where P_1, \dots, P_i are the first i oscillation periods. At those points the field will be of the form (3.16) with $a = a_{q.s.}$ determined by solving equation (3.17) for any given $r_p = r_{q.s.}(i)$. At each $r_{q.s.}$ we can determine the new value of ξ ,

$$\xi_{q.s.}(i) = \frac{\tilde{u}_\phi}{e^{a_{q.s.}/r_{q.s.}(i)} r_{q.s.}^2(i) \sqrt{-a_{q.s.}/(2r_{q.s.}^3(i))}} \quad , \quad (4.3)$$

the particle energy,

$$\tilde{u}^0 = \sqrt{e^{2a_{q.s.}/r_{q.s.}} + \tilde{u}_\phi^2/r_{q.s.}^2} \quad , \quad (4.4)$$

and the particle-field energy,

$$E = \frac{a_{q.s.}^2}{2r_{q.s.}} + m\tilde{u}^0 \quad (4.5)$$

We expect this to be a very good approximation for the particle energy at the true inversion points of the particle trajectory for a wide range of α 's and ξ 's (see figures 4.1 and 4.2). There usually is a value of ξ different from 1, ξ_o , at which

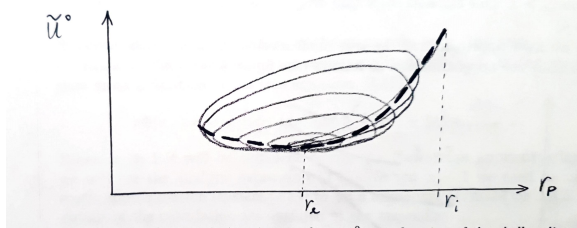


Figure 4.1: For the $\alpha \sim 1$, $\xi < 1$ case, shows \tilde{u}^0 as a function of the shell radius as expected from an exact numerical integration (solid line) and from the analytic expression (4.4) (dashed line). We expect the dashed curve to pass through the true values for the energy at the turning points of the particle orbit.

the energy of the particle in the final equilibrium state is equal to its energy at the

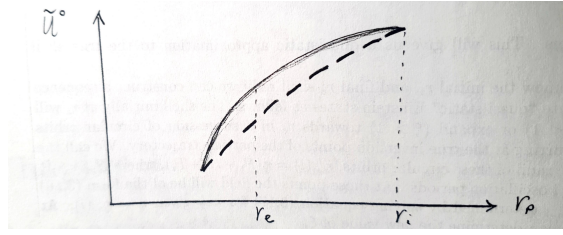


Figure 4.2: Same as figure 4.1 but for the $\alpha \gg 1$ and $\xi < 1$ case.

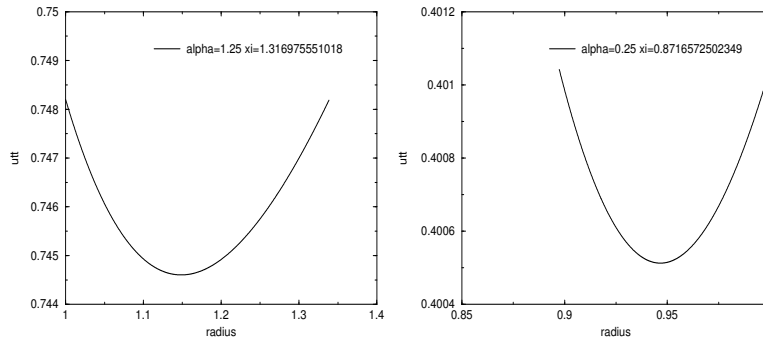


Figure 4.3: Shows \tilde{u}^0 as calculated from equation (4.4), as a function of the shell radius, for two different situations: on the left a more compact shell, on the right a less compact one.

beginning of the evolution (see figure 4.3). For shells with $\alpha < 0.4204623\dots$, $\xi_o < 1$, for less compact shells $\xi_o > 1$. One can also show that $E(r_{q.s.})$ has a minimum at $r_{q.s.}(\infty) = r_e$ (see figure 4.4).

Suppose we have approximated the true shell motion up to the i -th period P_i . Then we continue the approximation as follows (see figure 4.5),

1. Calculate $dE/dr_{q.s.}$ from equation (4.5),

$$\frac{dE}{dr_{q.s.}} = -\frac{a_{q.s.}^2}{2r_{q.s.}^2} + \frac{a_{q.s.}^3(5r_{q.s.} - 2a_{q.s.})}{r_{q.s.}(7a_{q.s.}r_{q.s.}^2 - 2a_{q.s.}^2r_{q.s.} - 4r_{q.s.}^3)} + m\frac{\tilde{u}_\phi^2}{\tilde{u}^0} \left(\frac{1}{\xi_{q.s.}^2 r_{q.s.}(7a_{q.s.}r_{q.s.}^2 - 2a_{q.s.}^2r_{q.s.} - 4r_{q.s.}^3)} - \frac{1}{r_{q.s.}^3} \right) \quad (4.6)$$

2. Calculate the energy radiated in the i -th oscillation period P_i . In general, when

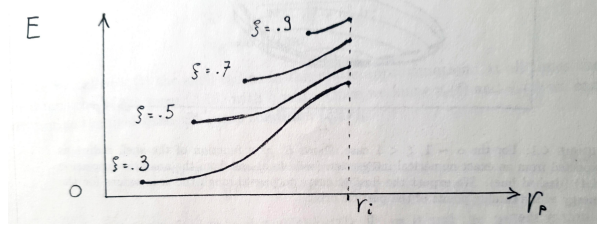


Figure 4.4: Shows the expected family of curves for E v.s. r_p parametrized by the particle's angular momentum ξ .

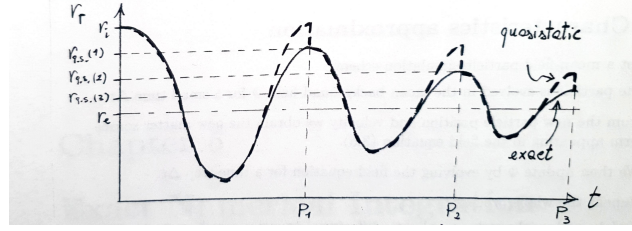


Figure 4.5: How the quasistatic approximation is expected to approximate a non-linear collapse.

$$r > r_p(t),$$

$$\Delta_{P_i} E = \int_{P_1 + \dots + P_{i-1}}^{P_1 + \dots + P_i} dt \frac{dE}{dt}, \quad (4.7)$$

$$\frac{dE}{dt} = \frac{1}{G} r^2 \Phi_{,t} \Phi_{,r} = -\frac{1}{G} (r \Phi_{,t})^2. \quad (4.8)$$

We need a good approximation to the monopole term (the lowest order contribution to the radiation) of the wave amplitude $r\Phi(r, t)$. In the weak field slow motion limit one finds (see equation (3.47)),

$$r\Phi(r, t) = -G \int dr' 4\pi r'^2 [\rho_0(\Phi - \frac{1}{2}v^2) + \frac{1}{6}r_p^2 \rho_{0,tt}]_{t-r}.$$

When $\alpha \gg 1$ it will be sufficient to use the Newtonian approximation. So we will use the analytic expression (3.61). When $\alpha \sim 1$ we need to use the static approximation (system (4.1)) to get a numerical estimate for $\Delta_{P_i} E$. The details of the calculation are outlined in the appendix.

3. Given $r_{q.s.}(i)$ we can find $r_{q.s.}(i+1)$ using the chain rule,

$$r_{q.s.}(i+1) = r_{q.s.}(i) + \frac{\Delta_{P_i} E}{dE/dr_{q.s.}(r_{q.s.}(i))}. \quad (4.9)$$

4. Start a new static oscillation from $r_i = r_{q.s.}(i + 1)$ and $\xi = \xi_{q.s.}(i + 1)$.

4.2 Characteristics approximation

We adopt a mean-field particle simulation scheme ¹:

1. The particle is evolved in the mean background field Φ for a small time Δt .
2. From the new particle position and velocity we obtain the new matter source term appearing in the field equation (3.6).
3. We then update Φ by evolving the field equation for a time-step Δt .
4. Repeat the whole process.

The particle evolves through an ordinary differential equation which poses no computational difficulties. One can for example use one of the standard Runge-Kutta schemes to solve it. The field evolution is much more problematic. It involves the solution of the Cauchy problem for a non-linear hyperbolic partial differential equation with discontinuous initial data. In the next chapter we will outline an exact numerical integration scheme for the field equation. Here we will describe an approximated one.

The idea is to use the auxiliary functions $X(r, t)$ and $Y(r, t)$ introduced in section 3.3. We make the following approximation: in the timestep dt we evolve the field according to equation (3.22) where we consider the source term F as constant in time ². Under this approximation, given at time t_o , $X(r, t_o) = X_o(r)$, and $Y(r, t_o) = Y_o(r)$ the solutions for X and Y at later times are,

$$\begin{aligned} X(r, t) &= X_o(r + \Delta t) - F \text{st}[r_p - \Delta t, r_p](r) + F \text{st}[-r_p - \Delta t, -r_p](r) , \\ Y(r, t) &= Y_o(r - \Delta t) + F \text{st}[r_p, r_p + \Delta t](r) - F \text{st}[-r_p, -r_p + \Delta t](r) , \end{aligned} \quad (4.10)$$

where $\text{st}[a, b](r) = H(x - a) - H(x - b)$ with H the Heaviside function, $\Delta t = t - t_o$, and we added an image source at $r = -r_p(t)$ ³ in order to ensure the finiteness of the field at the origin at all times, which requires,

$$X(0, t) = Y(0, t) \quad \forall t . \quad (4.11)$$

¹This scheme resembles Godunov's method used for the numerical solution of nonlinear systems of hyperbolic conservation laws [2]

²Note that this is an approximation even within the mean-field scheme since in its definition F contains the field itself.

³See appendix (B) for a justification of our use of the images method in the solution of this particular field equation.

We then reconstruct the gravitational field as follows,

$$\Phi(r, t) = \frac{1}{r} \int_0^r [X(r, t) + Y(r, t)] dr \quad . \quad (4.12)$$

In our code we tabulate the field using a uniform grid in r and we choose $dr = dt$. We need infact, to make sure that in using the solutions (4.10), the source terms fall upon the translated functions less frequently as possible. Those events are purely due to the mean field scheme, which require that we move the particle over a fixed field. When $dr = dt$ they occur only when the particle hits a grid point at a given timestep.

Chapter 5

Exact Numerical Integration

Here we describe the scheme we use to solve exactly the scalar field equation (3.6) coupled to the particle equations (3.9) in spherical symmetry, within the mean-field approximation described in section 4.2.

5.1 Characteristics method

In order to make the characteristics approximation an exact integration we need to replace the solution (4.10) with,

$$\begin{aligned} X(r, t) &= X_o(r + \Delta t) - F(r_p, t + (r - r_p))\text{st}[r_p - \Delta t, r_p] + \\ &\quad F(r_p, t + (r + r_p))\text{st}[-r_p - \Delta t, -r_p] \\ Y(r, t) &= Y_o(r + \Delta t) + F(r_p, t - (r - r_p))\text{st}[r_p - \Delta t, r_p] - \\ &\quad F(r_p, t + (r - r_p))\text{st}[-r_p, -r_p + \Delta t] \end{aligned} \quad (5.1)$$

In our numerical integration we have always used the field time-step Δt , equal to the particle time-step dt , equal to the grid spacing dr . In this case there is no difference in using equations (5.1) or (4.10). If we want to use $\Delta t = ndt$ with $n = 2, 3, \dots$ then the more general solution (5.1) should be used and solved by iteration.

5.2 High resolution method

A more rigorous method when computing discontinuous solutions of the wave equation can be found among the flux-limiter methods described in chapter 16 of Randall J. LeVeque “Numerical Methods for Conservation Laws”. Here we will describe the one employing the “Van Leer” smoother limiter function.

This method is second order accurate on smooth parts of the field and yet gives a well resolved, nonoscillatory discontinuity at the shell surface (by increasing the amount of numerical dissipation in its neighborhood). The method has the total variation diminishing property provided that the Courant, Friedrichs, and Lewy (CFL) condition is satisfied and consequently it is monotonicity preserving.

We will first state the method for a general linear hyperbolic system of partial differential equations and later specialize it to our nonlinear field equation.

Consider the time-dependent Cauchy problem in one space dimension,

$$\begin{aligned} u_{,t} + Au_{,x} &= 0 \quad , \quad -\infty < x < \infty \quad , \quad t \geq 0 \\ u(x, 0) &= u_o(x) \quad , \end{aligned}$$

where $u \in R^m$ and A is an $n \times n$ matrix. The system is called hyperbolic when A is diagonalizable with real eigenvalues, so that we can decompose $A = R\Lambda R^{-1}$, where $\Lambda = \text{diag}(\lambda_1, \lambda_2, \dots, \lambda_m)$ is the diagonal matrix of eigenvalues and $R = [r_1|r_2|\dots|r_m]$ is the matrix of right eigenvectors of A . Discretize time as $t_n = ndt$ and space as $x_j = jdr$. The finite difference method we want to describe produces approximations $U_j^n \in R^m$ to the solution $u(x_j, t_n) = u_j^n$ at the discrete grid points. The method is written in conservative form as follows,

$$U_j^{n+1} = U_j^n - \frac{dt}{dr}(FL_j^n - FL_{j-1}^n) \quad , \quad (5.2)$$

$$FL_j = FLL_j + FLh_j \quad , \quad (5.3)$$

$$FLL_j = \frac{1}{2}A(U_j + U_{j+1}) - \frac{1}{2}|A|(U_{j+1} - U_j) \quad , \quad (5.4)$$

$$|A| = R(\Lambda^+ - \Lambda^-)R^{-1}, \quad \Lambda^\pm = \text{diag}(\lambda_1^\pm, \dots, \lambda_m^\pm), \quad \lambda_p^\pm = \frac{\max}{\min}(\lambda_p, 0) \quad , \quad (5.5)$$

$$FLh_j = \frac{1}{2} \sum_{p=1}^m \phi(\theta_{pj})(\text{sgn}(\nu_p) - \nu_p)\lambda_p\alpha_{pj}r_p \quad , \quad (5.6)$$

$$\nu_p = \lambda_p \frac{dt}{dr} \quad , \quad (5.7)$$

$$\alpha_j = R^{-1}(U_{j+1} - U_j) \quad , \quad (5.8)$$

$$\phi(\theta) = \frac{|\theta| + \theta}{1 + |\theta|} \quad , \quad \text{“Van Leer” smoother limiter function} \quad (5.9)$$

$$\theta_{pj} = \frac{\alpha_{pj'}}{\alpha_{pj}} \quad , \quad j' = j - \text{sgn}\nu_p \quad (5.10)$$

FLh is the high order (Lax-Wendroff) flux acting on the smooth portions of the solution (where θ is near to 1) while FLL is the low order (first order upwind) flux acting in the vicinity of a discontinuity (where θ is far from 1). The CFL condition

is,

$$\left| \frac{\lambda_p dt}{dr} \right| \leq 1 \quad , \quad \forall p \quad . \quad (5.11)$$

Our field equation is a wave equation with a nonlinear source term. It can be rewritten as follows,

$$u_{,t} + Au_{,x} = b \quad , \quad (5.12)$$

$$u = \begin{pmatrix} u1 \\ u2 \end{pmatrix} = \begin{pmatrix} \Psi_{,x} \\ \Psi_{,t} \end{pmatrix} \quad , \quad \Psi(x, t) = x\Phi(x, t) \quad , \quad (5.13)$$

$$A = \begin{pmatrix} 0 & -1 \\ -1 & 0 \end{pmatrix} \quad , \quad |A| = \begin{pmatrix} 1 & 0 \\ 0 & 1 \end{pmatrix} \quad , \quad (5.14)$$

$$\Lambda = \begin{pmatrix} -1 & 0 \\ 0 & 1 \end{pmatrix} \quad , \quad R = \begin{pmatrix} 1 & 1 \\ 1 & -1 \end{pmatrix} \quad , \quad R^{-1} = \begin{pmatrix} 1/2 & 1/2 \\ 1/2 & -1/2 \end{pmatrix} \quad , \quad (5.15)$$

$$b = \begin{pmatrix} 0 \\ 4\pi G\sigma e^{\frac{1}{x}} \int_0^x u1(x', t) dx' x [\delta(x - r_p) + \delta(x + r_p)] \end{pmatrix} \quad . \quad (5.16)$$

$$(5.17)$$

The initial condition is,

$$u_o(x) = \begin{pmatrix} -a_i \text{st}[-r_i, r_i](x) \\ 0 \end{pmatrix} \quad . \quad (5.18)$$

If we call $r_{max} = j_{max} dr$ the maximum extent of our grid, the outgoing wave boudary conditions are,

$$\begin{aligned} u1(x > x_{max}, t) + u2(x > x_{max}, t) &= 0 \quad , \quad \forall t \quad , \\ u1(x < -x_{max}, t) - u2(x < -x_{max}, t) &= 0 \quad , \quad \forall t \quad . \end{aligned} \quad (5.19)$$

Imagine that we have approximated the true solution of the field equation up to the n-th time slice (i.e. we know U_j^n for $j = -j_{max}, \dots, -1, 0, 1, \dots, j_{max}$). The difference scheme,

$$U1_j^{n+1} = f(U1_{j-1}^n, U1_j^n, U1_{j+1}^n, U2_{j-1}^n, U2_j^n, U2_{j+1}^n) \quad , \quad (5.20)$$

$$U2_j^{n+1} = g(U1_{j-1}^n, U1_j^n, U1_{j+1}^n, U2_{j-1}^n, U2_j^n, U2_{j+1}^n) \quad , \quad (5.21)$$

when evaluated at j_{max} becomes a system of 2 equations in 2 unknowns $U1_{j_{max}}^{n+1}$ and $U1_{j_{max}+1}^n$,

$$U1_{j_{max}}^{n+1} = f(U1_{j_{max}-1}^n, U1_{j_{max}}^n, U1_{j_{max}+1}^n, U2_{j_{max}-1}^n, U2_{j_{max}}^n, U2_{j_{max}+1}^n) \quad , \quad (5.22)$$

$$U1_{j_{max}}^{n+1} = -g(U1_{j_{max}-1}^n, U1_{j_{max}}^n, U1_{j_{max}+1}^n, U2_{j_{max}-1}^n, U2_{j_{max}}^n, U2_{j_{max}+1}^n) \quad , \quad (5.23)$$

allowing the closure of the difference scheme. A consistency check would be to monitor the constraint,

$$U_0^n = 0 \quad , \quad \forall n \quad . \quad (5.24)$$

The difference scheme to be used for the field equation follows from equation (5.2),

$$U_j^{n+1} = U_j^n - \frac{dt}{dr} (FL_j^n - FL_{j-1}^n) + dt B_j^n \quad , \quad (5.25)$$

where B is the approximation to the source term b ,

$$B_j^n = \left(\begin{array}{c} 0 \\ 4\pi G\sigma(t_n) e^{\frac{1}{x_j} \int_0^{x_j} u1(x,t) dx} x_j \frac{W(r_p(t_n)-x_j)-W(-r_p(t_n)-x_j)}{dr} \end{array} \right) \quad . \quad (5.26)$$

In equation (5.26) we have approximated the delta functions using a triangular shaped cloud scheme, which in one dimension employs 3 mesh points and has an assignment-interpolation function W which is continuous in value and first derivative. Mass is assigned from the particle at r_p to the 3 mesh points nearest to it,

$$W(x) = \begin{cases} \frac{3}{4} - \left(\frac{x}{dr}\right)^2 & |x| \leq \frac{dr}{2} \\ \frac{1}{2} \left(\frac{3}{2} - \frac{|x|}{dr}\right)^2 & \frac{dr}{2} \leq |x| \leq \frac{3dr}{2} \\ 0 & \text{otherwise} \end{cases} \quad . \quad (5.27)$$

Chapter 6

Numerical results

When analyzing our numerical results, we will adopt gravitational units where $G = c = 1$. In this chapter we report the results obtained with the characteristic approximation code (see section D). We will refer to this results as the “exact integration” results.

6.1 Relaxation to virial equilibrium

When trying to reproduce the expected behaviour described in figure 3.4 we got figure 6.1.

When trying to reproduce the expected behaviour described in figure 3.1 we got figure 6.2.

6.2 Comparison with the analytic method

We compare the numerical integration in the linear and nonlinear regimes with the analytic Newtonian solution.

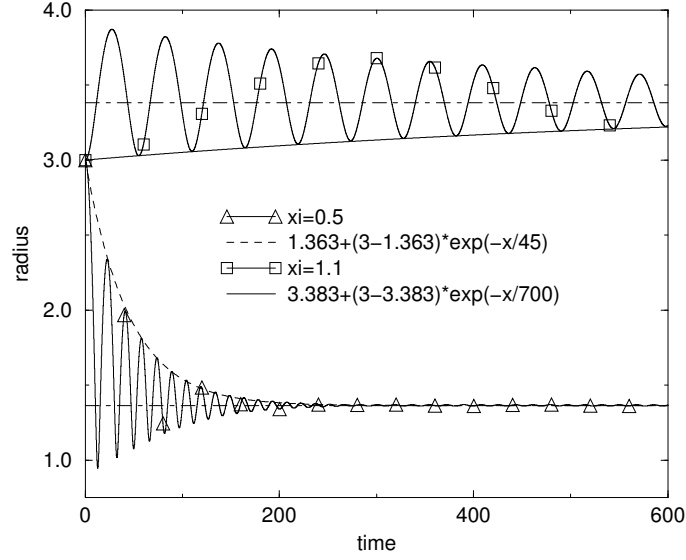


Figure 6.1: Shows the relaxation to the virial equilibrium state for an $\alpha = 3$ shell with two different values of ξ . In both cases the decay is fitted well by an exponential.

6.3 Monopole radiation

When trying to reproduce the expected behaviour described in figure 3.3 we got figure 6.6.

6.4 Quasistatic approximation

When trying to reproduce the expected behaviour described in figure 4.1 we got figures 6.7 and 6.8.

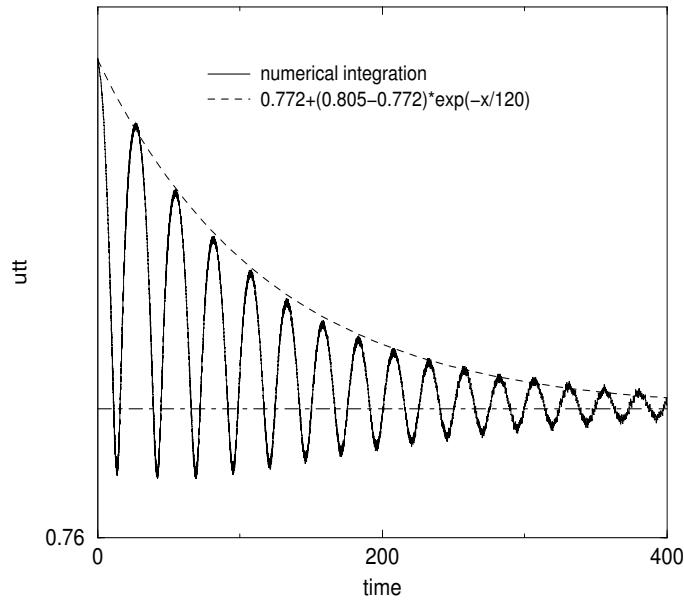


Figure 6.2: For the case $\alpha = 3$, $\xi = 0.7$ shows the particle energy \tilde{u}^0 versus time. The decay to the equilibrium value is well fitted by an exponential.

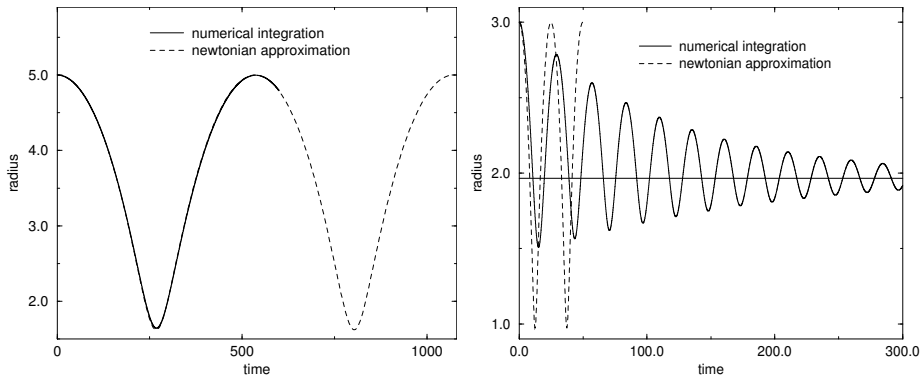


Figure 6.3: Compares the numerical integration with the analytic Newtonian approximation. To the left the quasi-Newtonian $\alpha = 500$, $\xi = 0.7$ shell is shown. The predicted equilibrium radius is at $r_e = 2.4662896500$. To the right the $\alpha = 3$, $\xi = 0.7$ shell is shown. The predicted equilibrium radius is at $r_e = 1.9657627134$.

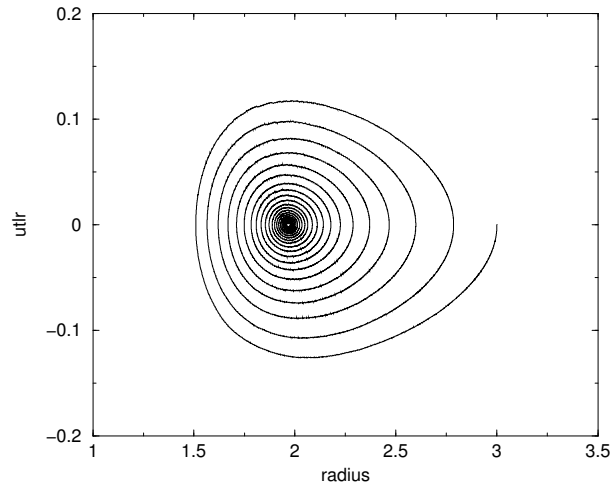


Figure 6.4: Shows \tilde{u}_r as a function of the shell radius for the case $\alpha = 3$, $\xi = 0.7$.

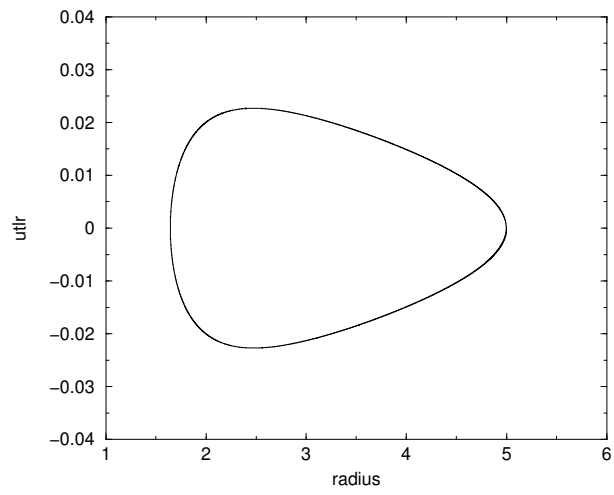


Figure 6.5: Same as figure 6.4 for the case $\alpha = 500$, $\xi = 0.7$.

Figure 6.6: For the case $\alpha = 3$, $\xi = 0.7$, shows a snapshot at $t=100$ of the field $\Phi(100, t)$, the first order radiation part (3.50), and the first order radiation part plus the zeroth order $-m/r$.

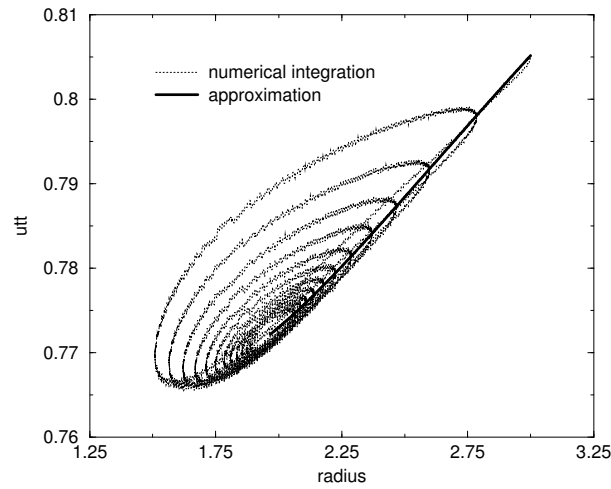


Figure 6.7: For the $\alpha = 3$, $\xi = 0.7$ case, shows the \tilde{u}^0 as a function of the shell radius for the numerical integration. The solid line was derived using the analytic expression (4.4). We see that it approximates well the values for the energy at the turning points.

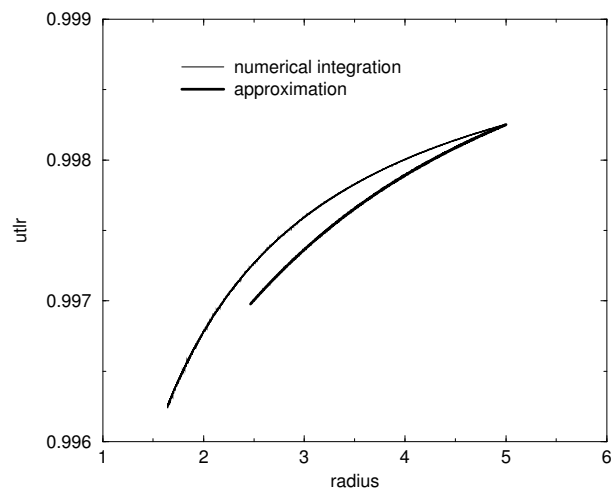


Figure 6.8: Same as figure 4.1 but for the $\alpha = 500$, $\xi = 0.7$ case.

Chapter 7

Conclusions

Some future developments to the present work may be:

- 0** Correct the characteristics approximation as outlined in section [refcharacteristics](#)
- 1** Integrate the equations (3.6) and (3.7) using the finite-difference scheme for the evolution of the field described in section 5.2.
- 2** Extend the one particle problem to a many particle one, and check how the quasistatic approximation performs there.
- 3** Go on to solve more realistic gravitational field theories, and look for quasistatic approximations.

Appendix A

Energy loss in the static approximation

In the weak field slow motion limit, in the wave zone the gravity wave amplitude can be written (dropping terms higher than the monopole) as (see equation (3.47) in the main text),

$$r\Phi(r, t) = -G \int dr' 4\pi r'^2 [\rho_0(\Phi - \frac{1}{2}v^2) + \frac{1}{6}r_p^2 \rho_{0,tt}]_{t-r} ,$$

where in the static approximation,

$$\rho_o = \frac{m}{4\pi r_s^2} \delta(r' - r_s) , \quad (\text{A.1})$$

$$v^2 = (\dot{r}_s)^2 + \left(\frac{\tilde{u}_\phi}{\tilde{u}^0} \right)^2 \frac{1}{r_s^2} , \quad (\text{A.2})$$

$$\Phi = \begin{cases} a_s/r_s & r \leq r_s \\ a_s/r & r > r_s \end{cases} , \quad (\text{A.3})$$

and $a_s = a_s(r_s, \tilde{u}_r)$ through the jump condition (see equation (4.2) in the main text),

$$a_s = - \frac{Gm e^{2a_s/r_s}}{\sqrt{e^{2a_s/r_s} + \tilde{u}_r^2 + \tilde{u}_\phi^2/r_s^2}} .$$

Then we can rewrite the wave amplitude as follows,

$$\begin{aligned} r\Phi(r, t) &= -Gm \left\{ \frac{a_s}{r_s} - \frac{(\dot{r}_s)^2}{2} - \left(\frac{\tilde{u}_\phi}{\tilde{u}^0} \right)^2 \frac{1}{2r_s^2} + \frac{1}{3}[(\dot{r}_s)^2 + r_s \ddot{r}_s] \right\}_{t-r} , \\ &= -Gm \left\{ \frac{a_s}{r_s} - \left(\frac{\tilde{u}_\phi}{\tilde{u}^0} \right)^2 \frac{1}{2r_s^2} - \frac{1}{6}(\dot{r}_s)^2 + \frac{1}{3}r_s \ddot{r}_s \right\}_{t-r} . \end{aligned} \quad (\text{A.4})$$

Taking the time derivative one gets (both \tilde{u}^0 and \tilde{u}_ϕ are constants of motion),

$$r\Phi_{,t} = -Gm \left\{ \frac{\dot{a}_s}{r_s} - \frac{a_s \dot{r}_s}{r_s^2} + \left(\frac{\tilde{u}_\phi}{\tilde{u}^0} \right)^2 \frac{\dot{r}_s}{r_s^3} + \frac{1}{3} r_s \ddot{r}_s \right\}_{t-r}. \quad (\text{A.5})$$

In the static approximation,

$$\dot{r}_s = \frac{\tilde{u}_r}{\tilde{u}^0}, \quad (\text{A.6})$$

$$\ddot{r}_s = \frac{\dot{\tilde{u}}_r}{\tilde{u}^0} = \left(\frac{\tilde{u}_\phi}{\tilde{u}^0} \right)^2 \frac{1}{r_s^3} - \frac{e^{2a_s/r_s}}{(\tilde{u}^0)^2} \frac{a_s}{2r_s^2}, \quad (\text{A.7})$$

$$\ddot{r}_s = - \left(\frac{\tilde{u}_\phi}{\tilde{u}^0} \right)^2 \frac{3\dot{r}_s}{r_s^4} - \frac{e^{2a_s/r_s}}{2(\tilde{u}^0)^2} \left(\frac{\dot{a}_s}{r_s^2} - \frac{2a_s \dot{r}_s}{r_s^3} \right) - \frac{e^{2a_s/r_s}}{(\tilde{u}^0)^2} \frac{a_s}{r_s^2} \left(\frac{\dot{a}_s}{r_s} - \frac{a_s \dot{r}_s}{r_s^2} \right) \quad (\text{A.8})$$

$$\dot{a}_s = (a_s)_{,\tilde{u}_r} \tilde{u}^0 \dot{r}_s + (a_s)_{,r_s} \dot{r}_s, \quad (\text{A.9})$$

$$(a_s)_{,\tilde{u}_r} = - \frac{\tilde{u}_r \frac{a}{e^{2a_s/r_s} + \tilde{u}_r^2 + \tilde{u}_\phi^2/r_s^2}}{1 - \frac{2a_s}{r_s} + \frac{a_s}{r_s} \frac{e^{2a_s/r_s}}{e^{2a_s/r_s} + \tilde{u}_r^2 + \tilde{u}_\phi^2/r_s^2}}, \quad (\text{A.10})$$

$$(a_s)_{,r_s} = - \frac{\frac{2a_s^2}{r_s^2} - \frac{a_s^2}{r_s^2} \frac{e^{2a_s/r_s}}{e^{2a_s/r_s} + \tilde{u}_r^2 + \tilde{u}_\phi^2/r_s^2}}{1 - \frac{2a_s}{r_s} + \frac{a_s}{r_s} \frac{e^{2a_s/r_s}}{e^{2a_s/r_s} + \tilde{u}_r^2 + \tilde{u}_\phi^2/r_s^2}}. \quad (\text{A.11})$$

Using equations (A.6)-(A.11) into equation (A.5) one can determine numerically the rate of energy loss (3.51). This can then be integrated to get the energy emitted by the particle in a full revolution around the origin. This calculation can be carried out analytically in the Newtonian approximation as shown in detail in the next section.

A.1 Newtonian approximation

In the Newtonian approximation we have,

$$a_s \rightarrow -Gm, \quad (\text{A.12})$$

$$\frac{\tilde{u}_\phi}{\tilde{u}^0} \rightarrow \sqrt{\frac{Gm\xi^2 r_i}{2}}, \quad (\text{A.13})$$

$$\ddot{r}_s \rightarrow -\frac{Gm}{2r_s^2} + \frac{Gm\xi^2 r_i}{2r_s^3}. \quad (\text{A.14})$$

Making these substitutions in equation (A.5) we get equation (3.59) of the main text,

$$r\Phi_{,t} = -\frac{4}{3} \frac{(Gm)^2}{r_i} \left[\frac{\dot{x}}{x^2} \right]_{t-r}, \quad (\text{A.15})$$

where $x = r_s/r_i$. So for the rate of energy emission in the wave zone we get equation (3.60), which integrated over one orbital period gives equation (3.61).

Appendix B

Method of Images

We want to justify the use we have made of the images method, in the solution of the nonlinear field equation (3.6).

To do that we need to show the equivalence between the two following problems. Calling $\Psi(r, t) = r\Phi(r, t)$, with $r \in [0, \infty]$, the first problem is our original one, namely,

$$\text{problem 1: } \begin{cases} \Psi_{,tt} - \Psi_{,rr} = F(r, \Psi(r, t))\delta(r - r_p) \\ \Psi(r, 0) = f(r) \\ \Psi_{,t}(r, 0) = 0 \\ \Psi(0, t) = 0 \\ \Psi_{,r}(r_m, t) + \Psi_{,t}(r_m, t) = 0 \end{cases} \begin{matrix} \text{i.c.} \\ \text{i.c.} \\ \text{b.c.} \\ \text{b.c.} \end{matrix} \quad (\text{B.1})$$

where i.c. stands for initial condition and b.c. for boundary condition.

The second problem is over the whole real axis $x \in [-\infty, \infty]$ and employs two sources, the one at r_p , of the first problem, and its image,

$$\text{problem 2: } \begin{cases} \Psi_{,tt} - \Psi_{,xx} = F(x, \Psi(x, t))[\delta(x - r_p) + \delta(x + r_p)] \\ \Psi(x, 0) = f(x) - f(-x) \\ \Psi_{,t}(x, 0) = 0 \\ \Psi_{,x}(\pm r_m, t) \pm \Psi_{,t}(\pm r_m, t) = 0 \end{cases} \begin{matrix} \text{i.c.} \\ \text{i.c.} \\ \text{b.c.} \end{matrix} \quad (\text{B.2})$$

The general solution to problem 1 can be written in integral form as follows,

$$\Psi(r, t) = \frac{1}{2}[f(r+t) + f(r-t) + W_{r_p}(r, t)] - \frac{1}{2}[r \rightarrow -r] \quad , \quad (\text{B.3})$$

where,

$$W_{r_p}(r, t) = \int_0^t d\bar{t} F(r_p, \Psi(r_p, \bar{t})) [H(r_p - r + (t - \bar{t})) - H(-r_p + r + (t - \bar{t}))] \quad (\text{B.4})$$

and the last term in equation (B.3) was added in order to have the solution satisfy the boundary condition at $r = 0$. The outgoing wave boundary condition is automatically satisfied since r_m is intended to be at all times to the right of the source, and $f(r)$ is constant for $r > r_p(0)$. So there are no ingoing waves passing through r_m .

The general solution to problem 2 can be written in integral form as follows,

$$\Psi(r, t) = \frac{1}{2} \{ [f(x+t) - f(-x-t)] + [f(x-t) - f(-x+t)] \} \quad (\text{B.5})$$

$$+ W_{r_p}(x, t) + W_{-r_p}(x, t) \} \quad , \quad (\text{B.6})$$

In order for the two problems to have the same solution for $x \geq 0$, the following condition has to be satisfied,

$$W_{r_p}(-x, t) = -W_{-r_p}(x, t) \quad . \quad (\text{B.7})$$

This condition is equivalent to,

$$F(r_p, \Psi(r_p, t)) = -F(-r_p, \Psi(-r_p, t)) = -F(-r_p, -\Psi(r_p, t)) \quad , \quad (\text{B.8})$$

where in the last equality we used the fact that the field is an odd function in x at all times. We can easily verify that our field equation, where,

$$F(r_p, \Psi(r_p, t)) = -\frac{Gm}{r_p} \frac{e^{2\Psi(r_p, t)/r_p}}{\sqrt{e^{2\Psi(r_p, t)/r_p} + \tilde{u}_r^2 + \tilde{u}_\phi^2/r_p^2}} \quad , \quad (\text{B.9})$$

satisfies such condition.

Appendix C

The nonhomogeneous wave equation

We want to find a solution to the following problem,

$$\Psi_{,tt} - \Psi_{,xx} = F(x, t) \quad , \quad (\text{C.1})$$

$$\Psi(x, 0) = 0 \quad , \quad (\text{C.2})$$

$$\Psi_{,t}(x, 0) = 0 \quad . \quad (\text{C.3})$$

Make the change of variables,

$$\xi = x + t \quad , \quad (\text{C.4})$$

$$\eta = x - t \quad . \quad (\text{C.5})$$

The differential equation then becomes,

$$\Psi_{,\xi\eta} \left(\frac{\xi + \eta}{2}, \frac{\xi - \eta}{2} \right) = -\frac{1}{4} F \left(\frac{\xi + \eta}{2}, \frac{\xi - \eta}{2} \right) \quad . \quad (\text{C.6})$$

Integrating with respect to ξ , we have,

$$\Psi_{,\eta} \left(\frac{\xi + \eta}{2}, \frac{\xi - \eta}{2} \right) = \Psi_{,\eta} \left(\frac{\xi + \eta}{2}, \frac{\xi - \eta}{2} \right) \Big|_{\bar{\xi}=\eta} \quad (\text{C.7})$$

$$+ \int_{\eta}^{\xi} \Psi_{,\xi\eta} \left(\frac{\bar{\xi} + \eta}{2}, \frac{\bar{\xi} - \eta}{2} \right) d\bar{\xi} \quad (\text{C.8})$$

$$= \frac{1}{2} \Psi_{,x}(\eta, 0) - \frac{1}{2} \Psi_{,t}(\eta, 0) \quad (\text{C.9})$$

$$- \frac{1}{4} \int_{\eta}^{\xi} F \left(\frac{\bar{\xi} + \eta}{2}, \frac{\bar{\xi} - \eta}{2} \right) d\bar{\xi} \quad (\text{C.10})$$

We integrate this equation from an arbitrary value of η to ξ to find,

$$\Psi(\xi, 0) - \Psi\left(\frac{\xi + \eta}{2}, \frac{\xi - \eta}{2}\right) = \int_{\eta}^{\xi} \left[\frac{1}{2} \Psi_{,x}(\bar{\eta}, 0) - \frac{1}{2} \Psi_{,t}(\bar{\eta}, 0) \right] d\bar{\eta} \quad (\text{C.11})$$

$$- \frac{1}{4} \int_{\eta}^{\xi} \int_{\bar{\eta}}^{\xi} F\left(\frac{\bar{\xi} + \bar{\eta}}{2}, \frac{\bar{\xi} - \bar{\eta}}{2}\right) d\bar{\xi} d\bar{\eta} \quad (\text{C.12})$$

In the first integral we note that,

$$\int_{\eta}^{\xi} \Psi_{,x}(\bar{\eta}, 0) d\bar{\eta} = \Psi(\xi, 0) - \Psi(\eta, 0) \quad . \quad (\text{C.13})$$

In the second integral we let,

$$\bar{\eta} = \bar{x} - \bar{t} \quad , \quad (\text{C.14})$$

$$\bar{\xi} = \bar{x} + \bar{t} \quad . \quad (\text{C.15})$$

The domain of integration $\eta \leq \bar{\eta} \leq \bar{\xi} \leq \xi$ becomes

$$\eta \leq \bar{x} - \bar{t} \leq \bar{x} + \bar{t} \leq \xi \quad , \quad (\text{C.16})$$

or

$$\eta + \bar{t} \leq \bar{x} \leq \xi - \bar{t} \quad , \quad 0 \leq \bar{t} \leq \frac{1}{2}(\xi - \eta) \quad . \quad (\text{C.17})$$

The jacobian determinant of the transformation from $(\bar{\xi}, \bar{\eta})$ to (\bar{x}, \bar{t}) is 2. Therefore

$$\frac{1}{4} \int_{\eta}^{\xi} \int_{\bar{\eta}}^{\xi} F\left(\frac{\bar{\xi} + \bar{\eta}}{2}, \frac{\bar{\xi} - \bar{\eta}}{2}\right) d\bar{\xi} d\bar{\eta} = \frac{1}{2} \int_0^{(\xi - \eta)/2} \int_{\eta + \bar{t}}^{\xi - \bar{t}} F(\bar{x}, \bar{t}) d\bar{x} d\bar{t} \quad . \quad (\text{C.18})$$

Making these substitutions and transposing, we find

$$\Psi\left(\frac{\xi + \eta}{2}, \frac{\xi - \eta}{2}\right) = \frac{1}{2} [\Psi(\xi, 0) + \Psi(\eta, 0)] + \frac{1}{2} \int_{\eta}^{\xi} \Psi_{,t}(\bar{x}, 0) d\bar{x} \quad (\text{C.19})$$

$$+ \frac{1}{2} \int_0^{(\xi - \eta)/2} \int_{\eta + \bar{t}}^{\xi - \bar{t}} F(\bar{x}, \bar{t}) d\bar{x} d\bar{t} \quad . \quad (\text{C.20})$$

We recall that $\xi = x + t$ and $\eta = x - t$. We use the initial conditions to obtain the solution formula

$$\Psi(x, t) = \frac{1}{2} \int_0^t \int_{x - (t - \bar{t})}^{x + (t - \bar{t})} F(\bar{x}, \bar{t}) d\bar{x} d\bar{t} \quad . \quad (\text{C.21})$$

The code

This is the code used for the exact numerical integration.

```

This is the code used for the exact
numerical integration.

cccccccccccccccccccccccccccccccccccccccccccccccccccccccccccc
c          1 SHELL CLUSTER
c
c dimt = number of timesteps in the integration
c dimg = dimension of the uniform r grid
c
c INPUT r0=shell radius
c        mr=shell rest mass
c        xi=up/up(circular)
c        dt=time-step
c        rot=dr/dt          dr=grid spacing
c OUTPUT
c        fort.8 = (t,rp)
c        fort.9 = (rp,utt,utlr)
c        erp=equilibrium radius
cccccccccccccccccccccccccccccccccccccccccccccccccccccccccccc
c        implicit none
c        include 'cluster.p'
c INPUT
c        real*8 r0,mr,xi
c        real*8 dt
c        integer rot
c OUTPUT
c        real*8 erp,rp,utt,utlr
c INTERNAL
c        real*8 phirp,e2p,fpl,fpr,phirpr,e2ppr,st
c        real*8 a,ea,dr
c        real*8 ut,up,utlp,am2
c        real*8 xx(0:imax),yy(-imax:imax)
c        real*8 rg(-imax:imax),phi(0:imax)
c        integer i,tsteps,jp,dimg,dimt
c        parameter(dimg=1000)
c        parameter(dimt=60000)
c =====INPUT DATA=====
c        call in(rp,mr,xi,dr,rot,dt)
c        r0=rp
c =====INITIAL CONDITION=====
c        tsteps=0
c -----uniform grid in r (spacing dr)-----
c        do i=-dimg,dimg
c            rg(i)=dble(i)*dr
c        enddo
c -----particle-----
c tangential orbit (utlr=0)
c        utlr=0.d0
c find angular velocity for the circular orbit at rp
c        call phil(mr,rp,a,up)
c angular momentum for circular orbits (in a time
c independent field) is:
c        utlp(circ)=ulp(circ)*exp(phi)=up(circ)*r*r*exp(phi)
c set utlp=xi*utlp(circ) = constant of motion
c        utlp=xi*rp**2*exp(a/rp)*up
c        am2 =utlp**2
c        up=utlp/(rp**2*exp(a/rp))
c        ut=sqrt(1.d0+(rp*up)**2)
c initial source term
c        st=exp(a/rp)*mr/(2.d0*rp*ut)
c -----field-----
c        xx(r,0)=yy(r,0)=(r*phi(r,0)),r
c phi(r,0)=a/r          r < rp
c phi(r,0)=a/r          r > rp
c        jp=nint(rp/dr)
c real space          r >= 0
c        do i=0,jp-1
c            xx(i)=.5d0*a/rp
c            yy(i)=.5d0*a/rp
c            phi(i)=a/rp
c        enddo
c        do i=jp,dimg
c            xx(i)=0.d0
c            yy(i)=0.d0
c            phi(i)=a/rg(i)
c        enddo
c imaginary space r < 0
c        do i=-dimg,-jp-1
c            yy(i)=0.d0
c        enddo
c        do i=-jp,-1
c            yy(i)=.5d0*a/rp
c        enddo
c =====NEXT TIMESTEP=====
100 tsteps=tsteps+1
c        if(mod(tsteps,rot).ne.0) goto 15
c -----evolve field-----
c reinterpolate phi(rp) to find new source term
c        jp =nint(rp/dr)
c        phirp=phi(jp)
c        e2p = exp(2.d0*phirp)
c        utt = sqrt(e2p*utlr**2+(utlp/rp)**2)
c the new source term is
c        st = .5d0*e2p*mr/(rp*utt)
c evolve the field
c        call evphi(dimg,dr,rg,st,rp,xx,yy,phi)
c -----evolve particle-----
c find e2p=exp(2*phi(rp))
15    jp = nint(rp/dr)
c        phirp = phi(jp)
c        e2p = exp(2.d0*phirp)
c find e2ppr=e2p*(phi,r(rp-)+phi,r(rp+))/2
c        fpl = (xx(jp-1)+yy(jp-1)-phirp)/rp
c        fpr = (xx(jp+1)+yy(jp+1)-phirp)/rp
c        phirpr= (fpl+fpr)*.5d0
c        e2ppr = e2p*phirp
c evolve the particle with 4-th order Runge-Kutta
c        call runge4(am2,e2p,e2ppr,dt,rp,utlr,rp,utlr)
c write fort.8 [:t,r(t)] and fort.9 [:t,utt(t),utlr(t)]
c        write(8,*) tsteps*dt,rp,phirp
c        write(9,*) rp,utt,utlr
c        if(tsteps.eq.dimt) goto 200
c        goto 100
c estimate the final equilibrium radius erp
200 call eqrp1(utlp,mr,erp,ea)
c write output
c        call out(mr,r0,erp,xi,dt,dr,dimt,dimg)
c
c stop

```



```

end

cccccccccccccccccccccccccccccccccccccccccccccccccccccccccccc
c Read initial data
c INPUT
c rp = initial shell radius
c mr = shell rest mass
c xi = ratio up/up(circular)
c dt = time-step
c rot = dr/dt(>=1 Courant stability condition)
c
c OUTPUT(all above +)
c dr = grid spacing
cccccccccccccccccccccccccccccccccccccccccccccccccccccccccccc
      subroutine in(rp,mr,xi,dr,rot,dt)
      implicit none
      real*8 rp,mr,xi,dr,dt
      integer rot

      write(*,*) 'initial radius rp'
      read(*,*) rp
      write(*,*) 'rest mass mr'
      read(*,*) mr
      write(*,*) 'ratio utlp/utlp(circular)'
      read(*,*) xi
      write(*,*) 'time-step dt'
      read(*,*) dt
      write(*,*) 'ratio dr/dt=[integer>=1]'
      read(*,*) rot
      dr=dt*double(rot)

      return
      end

cccccccccccccccccccccccccccccccccccccccccccccccccccccccccccc
c 4-th order runge-kutta
c advances to the next time step (h) the equations
c dr/dt=f(r,u)
c du/dt=g(r,u)
c where u=utlr (u tilde-low-r)
c f(r,u)=u/utu0
c g(r,u)=utlp**2/(utu0*r**3)-exp(2*phi)*phi,r/utu0
c utu0=sqrt(exp(2*phi)+u**2+(utlp/r)**2)
c and phi = potential at r,u
c phi,r = d(phi)/dr at r,u
c INPUT am2=(utlp**2 angular momentum squared),
c e2p(=exp(2*phi)),e2ppr(=exp(2*phi)*phi,r),
c h(=time step),ri,ui(=initial values for r,u)
c OUTPUT r,u (=final values for r,u)
cccccccccccccccccccccccccccccccccccccccccccccccccccccccccccc
      subroutine runge4(am2,e2p,e2ppr,h,ri,ui,r,u)
      implicit none
c INPUT
      real*8 am2,e2p,e2ppr,h,ri,ui
c OUTPUT
      real*8 u,r
c INTERNAL
      real*8 f,g,u0
      real*8 k1,k2,k3,k4,l1,l2,l3,l4
      real*8 k1o2,k2o2,l1o2,l2o2
      real*8 inv6
      parameter(inv6=1/6.d0)
      u0(r,u)= sqrt(e2p+u**2+am2/r**2)
      f(r,u)= u/u0(r,u)
      g(r,u)= am2/(u0(r,u)*r**3)-e2ppr/u0(r,u)

      k1 = h*f(ri,ui)
      l1 = h*g(ri,ui)
      k1o2= .5d0*k1
      l1o2= .5d0*l1
      k2 = h*f(ri+k1o2,ui+l1o2)
      l2 = h*g(ri+k1o2,ui+l1o2)
      k2o2= .5d0*k2
      l2o2= .5d0*l2
      k3 = h*f(ri+k2o2,ui+l2o2)
      l3 = h*g(ri+k2o2,ui+l2o2)
      k4 = h*f(ri+k3,ui+l3)
      l4 = h*g(ri+k3,ui+l3)

      r = ri+inv6*(k1+2.d0*(k2+k3)+k4)
      u = ui+inv6*(l1+2.d0*(l2+l3)+l4)

      return
      end

cccccccccccccccccccccccccccccccccccccccccccccccccccccccccccc
c Integrate the 1D wave equation with a delta
c function as the source
c -(r*phi),tt+(r*phi),rr=2*st*delta(r-rp)
c rewritten as
c xx,t=xx,r+st*delta(r-rp)
c yy,t=-yy,r-st*delta(r-rp)
c where
c xx=(v+w)/2
c yy=(v-w)/2
c and
c v=(r*phi),r
c w=(r*phi),t
c add an image to ensure finiteness of phi(0,t) forall t
c xx(0,t)=yy(0,t) at all times
c
c INPUT dr (= grid spacing), rg(-imax:imax) (= grid),
c st (= source term), rp (= shell radius),
c xxo(0:imax), yyo(-imax:imax) (= old "field")
c
c OUTPUT xxo(0:imax), yyo(-imax:imax), phi(0:imax) (=field)
cccccccccccccccccccccccccccccccccccccccccccccccccccccccccccc
      subroutine evphi(dimg,dr,rg,st,rg,xxo,yyo,phi)
      implicit none
      include 'cluster.p'
c INPUT
      integer dimg
      real*8 st,dr,rp
      real*8 rg(-imax:imax)
c OUTPUT
      real*8 xxo(0:imax),yyo(-imax:imax)
      real*8 phi(0:imax)
c INTERNAL
      real*8 xx(0:imax),yy(-imax:imax)
      real*8 dt,psi
      integer i

c check for rp>=rg(dimg-1)
      if(rp.ge.rg(dimg-1)) then
        write(*,*) 'particle out of right grid margin !!!'
        stop
      endif
c field timestep
      dt=dr
c yy(r)=yyo(r-dt)+st*step[rp,rp+dt]-st*step[-rp,-rp+dt]
c xx(r)=xxo(r+dt)-st*step[rp-dt,rp]
      yy(-dimg)=0.d0
      do i=-dimg+1,-1
        yy(i)=yyo(i-1)
        if(-rp.le.rg(i).and.rg(i).lt.-rp+dt) then
          yy(i)=yy(i)-st
        endif
      enddo
      do i=0,dimg-1
        xx(i)=xxo(i+1)
        yy(i)=yyo(i-1)
        if(rp-dt.le.rg(i).and.rg(i).lt.rp) then
          xx(i)=xx(i)-st
        elseif(rp.le.rg(i).and.rg(i).lt.rp+dt) then
          yy(i)=yy(i)+st
        endif
      enddo
      xx(dimg)=0.d0
      yy(dimg)=yyo(dimg-1)
c rewrite xx and yy
      do i=-dimg,-1
        yyo(i)=yy(i)
      enddo
      do i=0,dimg
        xxo(i)=xx(i)
        yyo(i)=yy(i)
      enddo
c integrate x+y starting from the origin
c using trapezoidal method (order dr**3)
      psi=.5d0*(xx(0)+yy(0))
      do i=1,dimg
        psi=psi+xx(i)+yy(i)
c the gravitational potential is
        phi(i)=dr*(psi-.5d0*(xx(i)+yy(i)))/rg(i)
      enddo

```

```

    phi(0)=phi(1)
c check boundary condition at r=0
    if(xx(0).ne.yy(0)) then
        print *, 'xx(0) <> yy(0) !!!!!!!'
    endif

    return
end

cccccccccccccccccccccccccccccccccccccccccccccccccccccccccccc
c Given rp (and ur=0) solves for a and up in:
c 1.0) ut = sqrt(1+ur**2+(rp*up)**2)
c 1.1) a = -exp(a/rp)*mr/ut
c 2) up = sqrt(-a/(2*rp**3))
c rewritten as
c -a = exp(a/rp)*mr/sqrt(1-a/(2*rp))
c
c INPUT mr (= rest mass), rp (= shell radius)
c OUTPUT a ("potential"), up (= angular velocity)
cccccccccccccccccccccccccccccccccccccccccccccccccccccccccccc
subroutine phi1(mr,rp,a,up)
    implicit none
c INPUT
    real*8 mr,rp
c OUTPUT
    real*8 a,up
c INTERNAL
    real*8 ao,sqti,ep,f,fp
    real*8 acc
    parameter(acc=1.d-15)

    a=0.d0
c start the Newton iteration
10 sqti=1.d0/sqrt(1.d0-a/(2.d0*rp))
    ep=exp(a/rp)
    f=a+mr*ep*sqti
    fp=1.d0+mr*ep*(sqti+.25d0*sqti**3)/rp
    ao=a
    a=ao-f/fp
    if(abs(f).gt.acc) goto 10

c the angular velocity rp*up**2=(a/rp**2)/2
    up=sqrt(-a/(2.d0*rp**3))
    return
end

cccccccccccccccccccccccccccccccccccccccccccccccccccccccccccc
c Finds the equilibrium radius
c given utlp solves for a and rp in:
c 1.0) utt = sqrt(exp(2*a/rp)+(utlp/rp)**2)
c 1.1) a = -exp(2*a/rp)*mr/utt
c 2) utlp**2=-exp(2*a/rp)*rp**3*(a/rp**2)/2
c rewritten as
c y=4*a**4/(a**4-(2*utlp*mr)**2)
c 1) utlp**2*(y/a**2)=-exp(y) -----> find a (<0)
c 2) r=(a**4-(2*utlp*mr)**2)/(2*a**3) -----> find r (>0)
c INPUT utlp (= angular momentum), mr (= rest mass)
c OUTPUT erp (= equil radius),ea (= equil "potential")
cccccccccccccccccccccccccccccccccccccccccccccccccccccccccccc
subroutine eqrp1(utlp,mr,erp,ea)
    implicit none
c INPUT
    real*8 mr,utlp
c OUTPUT
    real*8 ea,erp
c INTERNAL
    real*8 a4,y,ai,af,afo,fi,ff
    real*8 acc,u2,fu2m2
    parameter(acc=1.d-10)

    u2=utlp**2
    fu2m2=4.d0*u2*mr**2
c upper limit
    ai=0.d0
    fi=1
c find the lower limit
    af=-sqrt(2.d0*u2*(-1.d0+sqrt(1.d0+(-mr/utlp)**2)))
c start the secant iteration
10 a4=af**4
    y =4.d0*a4/(a4-fu2m2)
    ff=u2*y/af**2+exp(y)
    afo=af
    af=afo-ff*(afo-ai)/(ff-fi)
    if(abs((af-afo)/afo).gt.acc) then
        ai=afo
        fi=ff
        goto 10
    endif
c found a find r
    erp=(af**4-fu2m2)/(2.d0*af**3)
    ea =af

    return
end

cccccccccccccccccccccccccccccccccccccccccccccccccccccccccccc
c writes parameters in output
cccccccccccccccccccccccccccccccccccccccccccccccccccccccccccc
subroutine out(mr,ri,rf,xi,dt,dr,dimt,dimg)
    implicit none
    real *8 mr,ri,rf,dt,dr,xi
    integer dimt,dimg

c rest mass
    write(*,*) 'mr=',mr
c initial radius
    write(*,*) 'ri=',ri
c xi=up/up(circular)
    write(*,*) 'xi=',xi
c final equilibrium radius
    write(*,*) 'rf=',rf
c time step
    write(*,*) 'dtf=',dt
c grid spacing
    write(*,*) 'dr=',dr
c total integration time=dimt*dtf
    write(*,*) 'dimt=',dimt
c grid dimension r in [0,dimg*dr]
    write(*,*) 'dimg=',dimg

    return
end

```

This is the code used for enveloping the numerical integration.

end

```

cccccccccccccccccccccccccccccccccccccccccccccccccccccccccccc
c Relaxation to virial equilibrium
c
c INPUT  r0=shell initial radius
c        mr=shell rest mass
c        xi=up/up(circular)
c
c OUTPUT fort.10 : r_max,utt(r_max),xi
c          fort.14 : time,r_max
cccccccccccccccccccccccccccccccccccccccccccccccccccccccccccc
implicit none
c INPUT
  real*8  r0,mr,xi
c OUTPUT
  real*8  utt,r(0:1000),tt
c INTERNAL
  real*8  dr,dtdr(0:1000),etot,dedt,dedr
  real*8  a,ea,rf,utlp,up,am2
  real*8  e2p,npo2pi,xi2
  integer i,np
  parameter(np=999)
c =====INPUT DATA=====
  write(*,*) 'initial radius r0'
  read(*,*) r0
  write(*,*) 'rest mass mr'
  read(*,*) mr
  write(*,*) 'ratio utlp/utlp(circular)'
  read(*,*) xi
  if(xi.ge.sqrt(2.d0)) then
    print *, 'qust.f uses Newtonian approx. : xi < sqrt(2)'
    stop
  endif
c =====INITIALIZATION=====
c find angular velocity for the circular orbit at r0
  call phi1(mr,r0,a,up)
  utlp =xi*r0**2*exp(a/r0)*up
  am2 =utlp**2
c find final equilibrium radius rf and particle energy
  call eqrp1(utlp,mr,rf,ea)
  dr = (rf-r0)/dble(np)
  print *, 'initial radius, potential=',r0,a/r0
  print *, 'final radius, potential=',rf,ea/rf
  print *, 'initial energy utt=',sqrt(exp(2.d0*a/r0) +am2/r0**2)
  print *, 'final energy utt=',sqrt(exp(2.d0*ea/rf)+am2/rf**2)
c =====r_(max),xi,utt(r_(max))=====
  do i=0,np-1
    r(i)=r0+dble(i)*dr
    call phi1(mr,r(i),a,up)
    e2p=exp(2.d0*a/r(i))
    utt=sqrt(e2p+am2/r(i)**2)
c the new xi at r(i) is
    xi=utlp/(exp(a/r(i))*up*r(i)**2)
c write fort.10 : (r,utt,xi)
    write(10,*) r(i),utt,xi
c the total energy is then
    etot=mr*utt
    xi2=xi**2
c calculate detot/dr
    dedr=(a*r(i)*(4.d0-7.d0*xi2)+a**2*2.d0*xi2+r(i)**2*4.d0
      $ *(xi2-2.d0))/(xi2*r(i)**3*(7.d0*a*r(i)-2.d0*a**2-
      $ 4.d0*r(i)**2))
    dedr=mr*dedr*am2/utt
c calculate detot/dt
    npo2pi=sqrt(2.d0*r(i)**3/(a*(xi2-2.d0)**3))
    dedt=-(sqrt(2.d0)/9.d0)*mr**2*(sqrt(-a)**5/sqrt(r(i))**7)
    $ *((1.d0-xi2)**2/xi**7)*(5.d0-2.d0*xi2+xi**4)/npo2pi
c calculate dr/dt
    dtdr(i)=dedr/dedt
  enddo
c =====t,r_max=====
  write(14,*) 0,r0
c integrate (dt/dr) to get t(r)
  tt=.5d0*dtdr(1)
  do i=1,np-1
    tt=tt+dtdr(i)
c make graph (t(r),r)
    write(14,*) dr*(tt-.5d0*dtdr(i)),r(i)
  enddo
30 stop

```

This is the code used for the quasistatic integration.

```

Ccccccccccccccccccccccccccccccccccccccccccccccccccccccccccccc
c          1 SHELL QUASISTATIC CLUSTER
c
c INPUT rp=shell radius
c        mr=shell rest mass
c        xi=up/up(circular)
c        dt=integration timestep
c        time=simulation duration
c OUTPUT
c        fort.18 = (t,rp)
c        fort.19 = (rp,utt,utlr)
c        erp=equilibrium radius
cccccccccccccccccccccccccccccccccccccccccccccccccccccccccccc
c        implicit none
c INPUT
c        real*8 rp,mr,xi,dt,time
c OUTPUT
c        real*8 utlr,utt,erp,ea
c INTERNAL
c        real*8 am2,e2p,e2ppr
c        real*8 up,a,utlp
c        integer tsteps,dimt
c =====INPUT DATA=====
c        write(*,*) 'initial radius rp'
c        read(*,*) rp
c        write(*,*) 'rest mass mr'
c        read(*,*) mr
c        write(*,*) 'ratio utlp/utlp(circular)'
c        read(*,*) xi
c        write(*,*) 'time step dt'
c        read(*,*) dt
c        write(*,*) 'time lenght'
c        read(*,*) time
c        dimt=int(time/dt)
c =====INITIAL CONDITION=====
c        tsteps=0
c -----particle-----
c tangential orbit (utlr=0)
c        utlr=0.d0
c find angular velocity for the circular orbit at rp
c        call phi1(mr,rp,a,up)
c angular momentum for circular orbits (in a time
c independent field) is:
c        utlp(circ)=ulp(circ)*exp(phi)=up(circ)*r*r*exp(phi)
c set utlp=xi*utlp(circ) = constant of motion
c        utlp=xi*rp**2*exp(a/rp)*up
c        am2 =utlp**2
c -----field-----
c        phi(r)=a/rp for r<=rp
c        phi(r)=a/r for r> rp
c =====NEXT TIMESTEP=====
c        100 tsteps= tsteps+1
c            e2p=exp(2.d0*a/rp)
c find e2ppr=e2p*(phi,r(rp-)+phi,r(rp+))/2
c            e2ppr=-e2p*.5d0*a/rp**2
c -----particle-----
c evolve with 4-th order Runge-Kutta
c        call runge4(am2,e2p,e2ppr,dt,rp,utlr,rp,utlr)
c        if (rp.le.0.d0) then
c            print *,'particle fallen in to the origin !!!'
c            stop
c        endif
c -----field-----
c        call phi1(mr,rp,a,up)
c write fort.18 :[t,r(t)] and fort.19 :[t,utt(t),utlr(t)]
c        write(18,*) tsteps*dt,rp,a/rp
c calculate utt
c        utt=sqrt(e2p+utlr**2+am2/rp**2)
c        write(19,*) rp,utt,utlr
c        if(tsteps.eq.dimt) goto 200
c        goto 100
c estimate the final equilibrium radius erp
c        200 call eqrp1(utlp,mr,erp,ea)
c write erp and the field at erp (ea/erp)
c        print*,erp,ea/erp
c
c        stop
c        end

```


List of Figures

2.1	Pictorial evolution of the particle orbit when $J > 1$	6
2.2	Pictorial evolution of the particle orbit when $J < 1$	7
2.3	Expected behaviour for $\Phi(r_{out}, t)$ as a function of time.	8
2.4	Same as figure 2.3 but in the static approximation.	8
2.5	Shows the expected behaviour for the total energy of the system E as a function of the circular orbits radii R . The energy curve has its minimum at r_e , the radius of the circular orbit on which the particle decays at $t = \infty$	9
3.1	Shows the expected behaviour of the particle energy \tilde{u}^0 as a function of time for the case $\alpha \sim 1$ and $\xi < 1$	16
3.2	Energy conservation at two selected radii as a function of time. The solid line shows the left-hand side of equation (3.39) (volume integral plus integrated flux), the dotted line shows the second term alone (integrated flux), and the dashed line shows the right-hand side (volume integral at $t = 0$). The radii are (a) $r_{ec} < r_p(t)$ at all times, (b) $r_{ec} > r_p(t)$ at all times. The degree to which the solid and dashed lines coincide compared with the magnitude of the dotted line is a measure of the code's ability to conserve energy.	18
3.3	For the case $\alpha \sim 1$, $\xi < 1$, shows a snapshot at $t = t_o$ of the field $\Phi(t_o, r)$, the first order radiation part (3.50), and the first order radiation part plus the zeroth order $-m/r$	19
3.4	Shows the relaxation to the virial equilibrium state for an $\alpha \sim 1$ shell with two different values of ξ : $\xi < 1$ and $\xi > 1$	22
3.5	Expected shell behaviour for $\xi > \xi_e$	24
4.1	For the $\alpha \sim 1$, $\xi < 1$ case, shows \tilde{u}^0 as a function of the shell radius as expected from an exact numerical integration (solid line) and from the analytic expression (4.4) (dashed line). We expect the dashed curve to pass through the true values for the energy at the turning points of the particle orbit.	26

4.2	Same as figure 4.1 but for the $\alpha \gg 1$ and $\xi < 1$ case.	27
4.3	Shows \tilde{u}^0 as calculated from equation (4.4), as a function of the shell radius, for two different situations: on the left a more compact shell, on the right a less compact one.	27
4.4	Shows the expected family of curves for E v.s. r_p parametrized by the particle's angular momentum ξ	28
4.5	How the quasistatic approximation is expected to approximate a nonlinear collapse.	28
6.1	Shows the relaxation to the virial equilibrium state for an $\alpha = 3$ shell with two different values of ξ . In both cases the decay is fitted well by an exponential.	36
6.2	For the case $\alpha = 3$, $\xi = 0.7$ shows the particle energy \tilde{u}^0 versus time. The decay to the equilibrium value is well fitted by an exponential.	37
6.3	Compares the numerical integration with the analytic Newtonian approximation. To the left the quasi-Newtonian $\alpha = 500$, $\xi = 0.7$ shell is shown. The predicted equilibrium radius is at $r_e = 2.4662896500$. To the right the $\alpha = 3$, $\xi = 0.7$ shell is shown. The predicted equilibrium radius is at $r_e = 1.9657627134$	37
6.4	Shows \tilde{u}_r as a function of the shell radius for the case $\alpha = 3$, $\xi = 0.7$	38
6.5	Same as figure 6.4 for the case $\alpha = 500$, $\xi = 0.7$	38
6.6	For the case $\alpha = 3$, $\xi = 0.7$, shows a snapshot at $t=100$ of the field $\Phi(100, t)$, the first order radiation part (3.50), and the first order radiation part plus the zeroth order $-m/r$	39
6.7	For the $\alpha = 3$, $\xi = 0.7$ case, shows the \tilde{u}^0 as a function of the shell radius for the numerical integration. The solid line was derived using the analytic expression (4.4). We see that it approximates well the values for the energy at the turning points.	39
6.8	Same as figure 4.1 but for the $\alpha = 500$, $\xi = 0.7$ case.	40

Bibliography

- [1] S. L. Shapiro and S. A. Teukolsky. Scalar gravitation: A laboratory for numerical relativity. *Phys. Rev. D*, 47:1529, 1992. doi:10.1103/PhysRevD.47.1529.
- [2] S. K. Godunov. A Finite Difference Method for the Numerical Computation of Discontinuous Solutions of the Equations of Fluid Dynamics. *Mat. Sb.*, 47:271, 1959.